TECHNOLOGY MANAGEMENT AND ANALYSIS OF INTEGRATING FUEL CELL SYSTEMS IN GAS TURBINE POWER PLANTS

by

Nabil Omar Al Aid

A Thesis Presented to the Faculty of the
American University of Sharjah
College of Engineering
in Partial Fulfillment
of the Requirements
for the Degree of

Master of Science in
Engineering Systems Management

Sharjah, United Arab Emirates

April 2013

Approval Signatures

We, the undersigned, approve the Master's Thesis of Nabil Omar Al Aid
Thesis Title: Technology Management and Analysis of Integrating Fuel Cell Systems in Gas Turbine Power Plants.

Signature	**Date of Signature**
_____	_____
Dr. Mohamed Gadalla Professor, Department of Mechanical Engineering Thesis Advisor	
_____	_____
Dr. Ibrahim Al Kattan Professor, Engineering Systems Management Graduate Program Thesis Committee Member	
_____	_____
Dr. Essam Wahba Associate Professor, Department of Mechanical Engineering Thesis Committee Member	
_____	_____
Dr. Andreas Poullikkas Visiting Associate Professor, Department of Mechanical Engineering Thesis Committee Member	
_____	_____
Dr. Moncer Hariga Director, Engineering Systems Management Graduate Program	
_____	_____
Dr. Hany El Kadi Associate Dean, College of Engineering	
_____	_____
Dr. Leland Blank Interim Dean, College of Engineering	
_____	_____
Dr. Khaled Assaleh Director of Graduate Studies	

ACKNOWLEDGEMENTS

I wish to express my deepest gratitude to my supervisor Prof. Dr. Mohamed Gadalla for his valuable supervision, advice, encouragements and insight throughout the research. In addition, I gratefully thank him for creating an opportunity for submitting papers to ASME Fuel Cell Conference, 2010 and ASME Power Conference, 2013 which caused great motivation in advancing the thesis.

I would also like to thank all faculty members of the Engineering Systems Management Department for their instruction and advice during my graduate studies.

I also gratefully thank my wife and parents for their limitless support and encouragement for me in my entire life.

To My Wife and My Family

Abstract

In this thesis, comprehensive and detailed energy and economic analyses of integrating different types of fuel cells in gas turbine power plants are performed. The research investigates the performance of a hybrid system that consists of solid oxide fuel cells (SOFC) combined with a proton exchange membrane fuel cells (PEMFC) integrated into a gas turbine power plant. Detailed modeling including thermodynamic, kinetic, and geometric models are developed, implemented and validated for the synthesis/design and operational analysis of the combined hybrid system. In the proposed system, the PEMFC makes use of the internal reforming ability of the SOFC to produce hydrogen which is necessary for the PEMFC operation. A detailed comparative study between the proposed system and other conventional or SOFC integrated systems is also conducted. The comparative study includes performing a complete technical and economic study for each of the proposed systems which are the conventional gas turbine cycle, the SOFC-gas turbine integrated cycle (SOFC-GT), and the PEMFC, SOFC and gas turbine integrated cycle. Different levels of modeling for the SOFC, the PEMFC and the integrated system are presented. The study also includes applying different methods and techniques to enhance the efficiency of the proposed cycle. The efficiency of the plant is studied by varying several parameters including operating pressure for the SOFC-GT system, temperatures of the fuel and the air, and the mass flow rates of air and fuel. Energy and entropy balances are performed not only for the overall systems but also for each component of the systems to evaluate performance of each system in addition to the distribution of irreversibility and thermodynamic inefficiencies. Furthermore, a detailed exergy analysis is conducted for each of the proposed systems under investigation. This analysis is achieved by calculating the exergy destruction and exergetic efficiency for each component in each of the investigated systems. Finally, the analysis also shows detailed calculations of the overall second law efficiency as well as detailed economic analysis of the proposed integrated systems.

Keywords: Gas Turbine Power Plant, PEM fuel cell, SOFC, Exergetic Efficiency, Thermal Efficiency, Economic Analysis, Technology Management.

Table of Contents

List of Figures

List of Tables

Abbreviations

A	cell active area (cm2)
c_p	specific heat (kJ/kg K)
e_{xch}	molar-specific chemical exergy (kJ/kmol)
e_{xph}	mass-specific physical exergy (kJ/kg)
E	energy flow rate (kW)
E_{xd}	exergy destruction rate (kW)
F	Faraday's constant (96,439 C/moles of electrons)
g	Gibbs-specific molar energy (kJ/kmol)
h	specific enthalpy (kJ/kg)
i	current density (mA/cm2)
i_l	limiting current density (mA/cm2)
i_n	internal current density (mA/cm2)
i_0	exchange current density (mA/cm2)
I	current (A)
i_n	internal current density (mA/cm2)
L	mechanical power (kW)
m	mass flow rate (kg/s)
M	molar mass (kmol/kg)
n	molar flow rate (mol/s)
n_e	number of moles of electrons per mole of H_2 reacted
p_{ref}	reference pressure (1 bar)
Q	heat flow rate (kW)
R	molar gas constant (8.31 kJ/kmol)
s	specific entropy (kJ/kg K)
S_{gen}	entropy generation rate (kW)
t	temperature (1C)
T	temperature (K)
U_f	fuel utilization factor
V_E	cell voltage (V)

x methane reforming rate of reaction

y shift rate of reaction

z electrochemical rate of reaction

z number of moving electrons

E_n Nernst voltage

i_0 exchange current

α charge transfer coefficient

P_{Fuel} absolute supply pressure of fuel (atm)

P_{air} absolute supply pressure of air (atm)

V_{lpm} flow rate (l/min)

x percentage of hydrogen in the fuel (%)

y percentage of oxygen in the oxidant (%)

P_{H2} partial pressure of hydrogen inside the stack

P_{O2} partial pressure of oxygen inside the stack

P_{H2O} partial pressure of water vapor inside the stack

k Boltzmann's constant = J/0K

h Planck's constant = J s

ΔG size of the activation barrier which depends on the type of electrode and catalyst used

η_{nom} nominal LHV efficiency of the stack (%)

V_{nom} nominal voltage (V)

ACC annual capital cost, $/kW yr

CRF capital recovery factor, yr−1

CF capacity factor

I_r interest rate, %

N_y fuel cell lifetime, yr

C exergetic cost, $/GJ

CO&M annual cost of operation and maintenance of fuel cell, $/kW yr

CFC fuel cell cost, $/kW

CW cost of exergetic power of fuel cell, $/GJ

E total exergy per unit mass, k J/kg

$\dot{E}$	total exergy rate, kW
$\dot{m}$	mass flow rate, kg/s
$\dot{W}$	electrical power output, kW
T	temperature, K
T_o	standard temperature, 288 K
P	pressure, atm
P_o	standard pressure, 1 atm
V	cell voltage, Volts
ZFC	total investment cost of fuel cell, $/s

Chapter 1: Introduction

1.1 Project Background

It is becoming extremely critical to develop new energy systems with renewable fuels, reduced environmental impact and high efficiency in order to meet the rising demand of energy and to preserve the global environment. It is well known that using fossil fuels in power generation systems creates many environmental issues, mainly because of the emission of polluted and greenhouse gases into the atmosphere. Hydrogen is one of the best available options to be used as a green fuel. However, it requires a major technological and research effort to solve the issues related to storage and transportation. Until a solution is in place, using the alternative carriers of the hydrogen energy like coal and natural gas could contribute to the successful transition into the "hydrogen economy." A wide range of fossil fuel and renewable energy sources can produce these alternative energy carriers[1]. The advantage of these energy carriers is the fact that they can be easily handled and that they can be fed into many energy conversion systems, like fuel cells and gas turbine cycles, with high efficiency and low greenhouse emissions. Accordingly, one of the most promising technologies in the market is the fuel cell due to its high efficiency and environmentally-friendly operation.

Economically, the fuel cell market hasn't grown for several years and remained stable at around $100M USD. This is mainly due to the relatively high cost per each kilowatt comparing to the existing utility technologies. With the rising prices of fuel, the growing environmental concerns, and the intensive demand for reliable energy sources, the fuel cell market is becoming more mature. As a matter of fact, demonstrating 2-meagawatt fuel cell power plants helps to study the feasibility of the R&D of fuel cells.

Commercialization of an energy source necessitates sustainability and high efficiency of the proposed source. The analysis of the fuel cell companies indicates that the target cost is $300 per kilowatt to make the fuel cells commercially available. However, currently the fuel cell costs around $2,000 to $3,500 per kilowatt [1]. On the other hand, economies of scale and the introduction of new manufacturing material are needed to meet the target costs.

1.2 Objectives and Problem Statement

1.2.1 Objectives

The main objective of this thesis is to develop an understanding of the economic, technology, and marketplace drivers needed for commercialization of stationary fuel cell systems.

In addition to this, this thesis aims to enhance the performance and improve the efficiency of a gas turbine cycle by integrating SOFC and PEMFC fuel cells with the combined cycle

1.2.2 Problem Statement

Study the performance of the proposed system and perform modeling and simulation for each of the system components and analyze the system economically and commercially. In addition to this, compare the proposed system with other similar systems and perform an economic and technical evaluation for each of the proposed systems.

1.3 Theoretical Background

1.3.1 Low- and Medium-Temperature Fuel Cells

A complete range of fuel cells are available that can be classified by the electrolyte and operating temperatures. All the different types of fuel cells operate in a similar manner. The fuel enters the fuel cell at the anode and is then oxidized and separated into protons and electrons. While the air enters at the cathode, the oxygen is reduced. Either the protons or the oxygen ions travel through the electronically-insulated ion-conductor to combine with other ions or protons to generate water and electricity[3].

To study the performance of the Polymer Exchange Membrane Fuel Cells (PEMFC) and understand its operation, it is important to understand its principal of operation and the physical structure. ‘A PEM fuel cell consists of two electrodes with a thin layer of catalyst in contact with a plastic membrane separating gas supply chambers’[4]. Hydrogen gas (H_2) which acts as fuel, having its source from methanol (CH_3OH), petroleum products, or natural gas, is fed through a narrow channel from one

end of the plate (anode). Similarly, oxygen (O_2) enters the fuel cell from the other end of the plate (cathode). Figure 1 represents a schematic diagram of a polymer electrolyte membrane fuel cell [3].

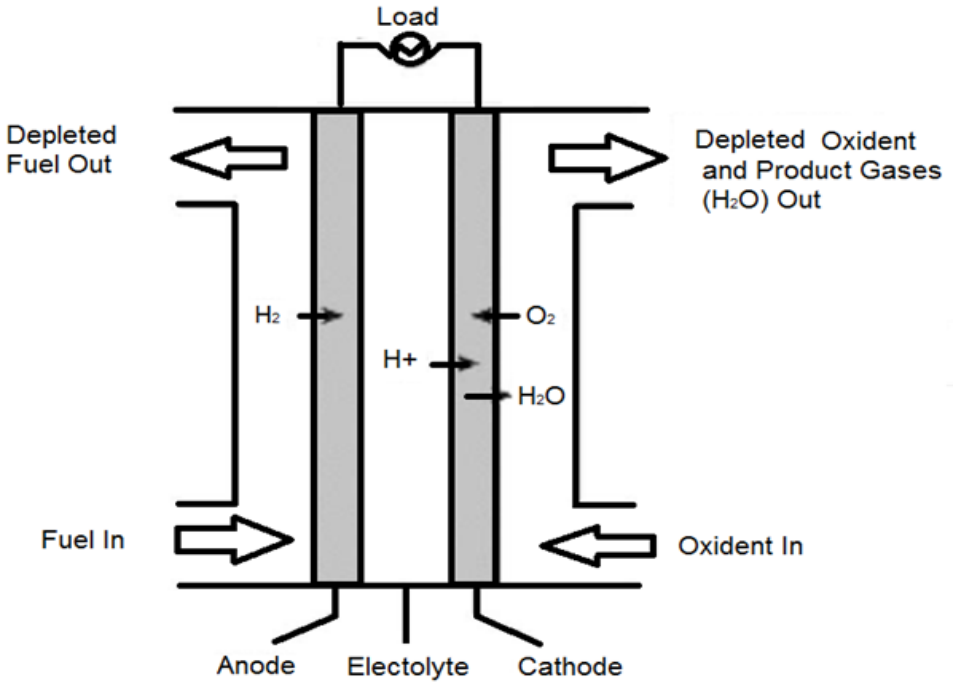

Figure 1: PEMFC Schematic Diagram [1]

1.3.2 High-Temperature Fuel Cells

There two common types of high temperature fuel cells which are solid oxide and molten carbonate (SOFC and MCFC). Both types have been mainly considered for large-scale (MW) stationary power generation. In these systems, the electrolytes consist of anionic transport materials, as O_2 and CO_2 are used as the charge carriers. These two types of fuel cells have two major advantages over low-temperature types. First, they can achieve high electric efficiencies, as prototypes have achieved over 60%[1]. This makes them particularly attractive for fuel-efficient stationary power generation. The second main advantage is the fact that the high operating temperatures allow direct internal processing of common fuels such as natural gas. This reduces the system complexity compared with low-temperature power plants, which require hydrogen generation in an additional step in the process. However, the fact that the high temperature fuel cells cannot easily be turned off is acceptable in the stationary sector, but most likely only there.

1.4 Literature Review

Hoogers [1] provided a comprehensive and detailed introduction to different types of fuel cells and how to use them in real life applications. His book includes current developments in manufacturing, integrating, and engineering economics relevant to the fuel cell systems. The use of high temperature and low temperature fuel cells is also highlighted. Detailed descriptions of engineering economics and thermo-economics are also presented. Moreover, a case study is considered throughout the book for continuity of the presentation. The case study involves the design of a gas turbine integrated system.

Cengel [2] presented a methodology for performance evaluation of a combined-cycle cogeneration system. Energy balances and performance assessment parameters of that system are given in his study. Results for such a system using an advanced gas turbine as the prime mover show that it is a very versatile system. It can produce a large power-to-heat ratio together with high second-law efficiency over a wide range of process steam pressures.

Ma et al. [3], and Zhang et al. [4] focused in their studies on the feasibility and future of fuel cell technology and highlight the major challenges in adopting this technology.

Yi et al. [5] represented a theoretical understanding and thermodynamic simulation capability for investigation of an integrated SOFC reformer system operating on various fuels. The theoretical understanding and simulation results suggest that significant thermal management challenges may result from the use of different types of fuels in the same integrated fuel cell reformer system.

Haseli et al. [6], Tanaka et al. [7], Yerramalla et al. [8], and Spiegel [9] studied the performance of various fuel cell integrated systems in gas turbine cycles. Their research work show a detailed first law analysis of the integrated systems and study the behaviors of the systems at different operating conditions.

Chan et al. [10] focused on a natural gas-fed integrated internal-reforming solid oxide fuel cell–gas turbine (IRSOFC–GT) power generation system. The analyzed

system shown in their study consists of a fuel compressor and an air compressor, an SOFC stack, an integrated reformer, a combustor, a gas turbine and a power turbine, and a heat recovery steam generator (HRSG). Different levels of modeling work for the fuel cell, fuel cell stack, and integrated system were conducted, which provided a means of sizing up the power system in the developmental stage. Based on the obtained simulation results the IRSOFC–GT power system could achieve a net electrical efficiency of better than 60% and a system efficiency of better than 80%.

Winter [11], Avadikyan et al. [12], Bompard et al. [13], Ang et al. [14], Lipman et al. [15], and Agnolucci [16], performed a study on the economic feasibility of integrated fuel cell systems. Their studies show various equations and methods to estimate the capital cost, the operation and maintenance cost and the replacement cost of the fuel cells. In addition to this, these studies show the procedure to do perform a detailed economic feasibility of integrated fuel cell systems. Furthermore, the studies describe the methods to perform the economic analyses over the lifetime of the fuel cells and the ways to calculate the Net Present Value (NPV) for the integrated systems.

Barbir et al. [17] performed the analysis of the efficiency and economics of the fuel cells in various load profiles and for various development and cost scenarios. The results obtained indicate that in the best case scenario the fuel cells can be produced at $l00/kW, operate at 50% efficiency, and generate electricity at 100$/kWh if hydrogen can be supplied at $10/GJ.

Cheddiea et al. [18] developed a thermo-economic model to optimize an indirectly coupled SOFC–GT hybrid power plant. Indirect coupling was utilized because it offers the most practical coupling of SOFCs to existing GT power plants. The obtained results show that the overall thermal efficiency can be increased from 30% to 48% while the cost of producing power can be reduced from 5.46 to 4.65 $/kWh as a result of the coupling. The most optimum performance was observed when a 11MW SOFC was used for a total power output of 20.6MW. Sensitivity analyses also showed that for indirectly coupled SOFC–GT hybrid applications, it is preferable to operate the SOFC at a cell voltage of 0.5 V, to utilize low air flow rates and 60% anode recycling.

Kazim [19] performed a comprehensive exergoeconomic analysis of a 10 kW PEM fuel cell at various operating temperatures, pressures, and cell voltages. The analysis was performed at fuel cell operating temperatures (T/T_o) and pressures (P/P_o) ranging from 1 to 1.25 and 1 to 3, respectively. The calculated results showed the significance of the operating pressure and cell voltage on the exergy cost of the fuel cell. Furthermore, the economic feasibility of fuel cell relies on a lower capital cost of the fuel cell, annual operation and maintenance cost and hydrogen cost. Thus, a substantial improvement in the overall results could be achieved.

Sreeramulu et al. [20], Baheta et al. [21] and Jubeh [22] performed a detailed exergy analyses for gas turbine cycles. Their research shows the procedure to perform the exergy analysis and develop the understanding of the importance of performing this analysis. All the required equations to estimate the exergy analyses including exergy calculations for compressor, heat exchangers, gas turbines and combustors are explained in these studies. In addition to this, the method to calculate the second law efficiency for each component and for the overall system is also described.

Ghanbari [23] analyzed methane-fed internal reforming solid oxide fuel cell–gas turbine system based on the first and second law of thermodynamics. In his work exergy analysis is performed to estimate the losses in each component. The proposed system consists of a fuel compressor and air compressor, a pre-reformer, a SOFC stack, a combustor, a gas turbine and a heat recovery steam generator. A parametric study is also performed to evaluate the effect of various parameters such as air flow rate, fuel flow rate, temperature and pressure on system performance.

Haseli et al. [24], Hotz et al. [25], Hussain et al. [26] and Akkayaa et al. [27] performed a detailed second law analyses for various integrated systems. Their studies show comparative analyses based on the exergy destruction calculations and based on the second law efficiencies. Their work also shows various methods to perform detailed chemical and physical exergy calculations for both PEMFC and SOFC stacks.

Hotz et al. [28] applied an exergy analysis on a combined system which consists of a steam reformer fed by methanol and a direct methanol fuel cell (DMFC) micro-

power plant combined with a hydrogen polymer electrolyte fuel cell (PEFC) micro-power plant. The influence of significant operational parameters on the exergetic efficiency is examined numerically in their work. Experimental results are conducted for the steam reformer. This work shows the importance of performing exergy analysis of the fuel cell as part of an entire thermodynamic study and compares the two different power plants based on their exergitc efficiencies.

Calise et al. [29] discussed the simulation and exergy analysis of a hybrid solid oxide fuel cell–gas turbine (SOFC–GT) power system. In their study, the energy and exergy balances are performed not only for the whole plant but also for each component in order to evaluate the distribution of irreversibility and thermodynamic inefficiencies. Simulations are performed for different values of fuel utilization factor, operating pressure, and current density. Results showed that, for a 1.5MW system, an electrical efficiency close to 60% can be achieved. When heat loss recovery is also taken into account, a global efficiency of about 70% is achieved.

Kazim [30], Schootsa et al. [31], Ang et al. [32], Winter [33], Zegers [34], Sopiana et al. [35], Barrett [36], Hart [37] and Wee [38] discussed various methods to optimize the performance of the fuel cells and enhance its efficiency. The authors investigated the issues and the challenges in the commercialization of fuel cells and their integration with power plants. These challenges include the high manufacturing cost, the storage of hydrogen and the operation and maintenance cost. Furthermore, these studies also discuss main success factors which contribute to the success of the fuel cell technology and the future enhancements required to adopt the technology. Finally, the studies also propose different applications for the fuel cell technology including integration with various systems in the field of transportation and power generation.

1.5 Significance of Thesis

For almost a decade many researchers have studied the performance of an integrated SOFC in the gas turbine power generation cycle in order to enhance the system performance and to increase the efficiency. The researchers have proposed replacing the combustion chamber with the SOFC as a major source of heating energy; they have also

proposed utilizing the ideal operating conditions to generate electrical power from the SOFC. In particular, as the operating temperature of solid oxide fuel cells (SOFC) ranges from 800 ^{0}C to 1000 ^{0}C, the SOFC stack can replace the combustion chamber of conventional micro gas turbines (MGT). These hybrid SOFC–MGT power plants are a very attractive near-term option as they can achieve efficiencies of over 60–65%, even for small power outputs (200–400 kW). Another important factor is that using an integrated cycle will help reduce the CO emissions because of the internal reforming process in the SOFC.

This thesis proposes integrating an additional type of fuel cells which is the PEMFC in the SOFC-GT hybrid system. The main reason for introducing the medium temperature PEMFC is the fact that the excess hydrogen produced inside the SOFC stack is not utilized, and this hydrogen can be utilized as a fuel for the PEMFC stack to produce additional electrical power.

1.6 Technology Management of Fuel Cells

1.6.1 Performance Optimization & 1st Law Analysis of the integrated systems

In this section of the thesis, a detailed technical analysis is performed including modelling of the integrated systems, identifying the configuration parameters of each of the system components, simulating each of the systems at different operating conditions, and finally optimizing the performance of the systems under study. In addition to this, the calculations of the output power and thermal efficiency are also shown in this section.

1.6.2 2nd Law Analysis of the integrated system

Energy and exergy balances are to be performed not only for the whole plant but also for each component in order to evaluate the distribution of irreversibility and thermodynamic inefficiencies. Simulations are to be performed for different values of operating pressure, fuel utilization factor, fuel-to-air and steam-to-fuel ratios, and current density.

1.6.3 Economic Analysis of Fuel Cells

A complete study is done to analyze the economic effect of applying such a technology in real-life power generation. This study shall include the initial cost of implementing the solution in addition to the return on investment period. Furthermore, the analysis will include study on how to further reduce the cost by introducing new technologies like pulse combustors and using different types of fuels.

The overarching objective of this thesis is to drive the Research &Development needed for the commercialization of the fuel cell system by improving and expanding our understanding of the economic, technical, and market factors. Outcomes of this study include a technical targets table showing cost, efficiency, and profitability for each of the proposed systems. In addition major challenges for fuel cell applications are also identified and evaluated to determine critical success factors required for commercialization.

Figure 2 below shows the steps to be followed to perform the technology management of the proposed system.

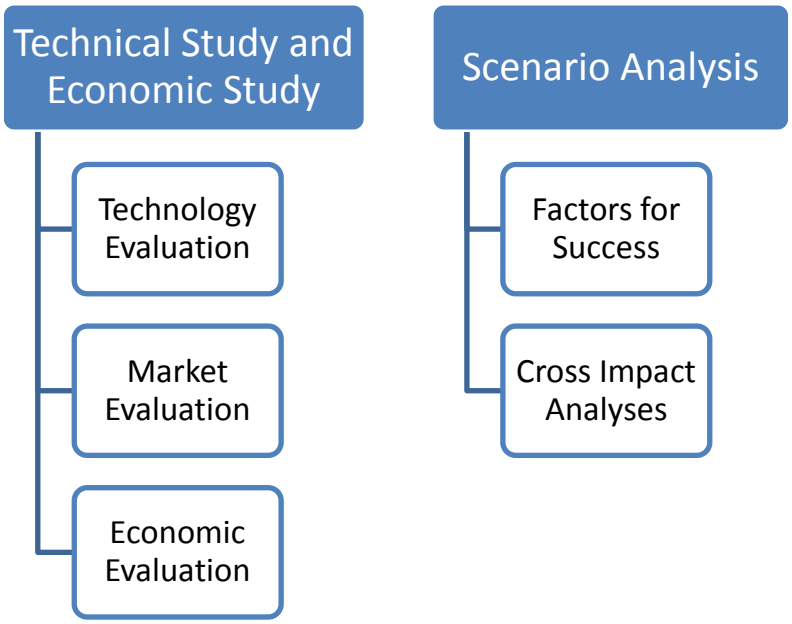

Figure 2: Technology Management of the Proposed System

1.6.4 Comparison with Other Similar Systems

After doing the complete technical management and economic evaluation of the complete system, a comparison will be done with other systems to highlight the proposed system advantages and disadvantages comparing to the other systems. The following systems will be also evaluated and tested:

- Conventional gas turbine system with a combustion chamber
- Integrated SOFC stack into a gas turbine system
- The proposed integrated system with both SOFC and PEMFC

1.7 Proposed System Description

1.7.1 Schematic diagram of the proposed system

Figure 3 shows the proposed system layout. As shown, the model suggests the use of two compressors, an air compressor and a fuel compressor. The compressed heated air flows to the cathode of an SOFC for oxygen reduction. Since the net chemical process in the SOFC is exothermic, both the air and fuel temperatures increase through the flow chambers of the SOFC. The SOFC stack produces electrical power together with an exhaust stream that contains unused CH_4 and H_2. The SOFC exhaust stream is routed to a PEMFC where it is cooled to the PEMFC standard operating temperature and produces electrical power using the H_2 as a fuel.

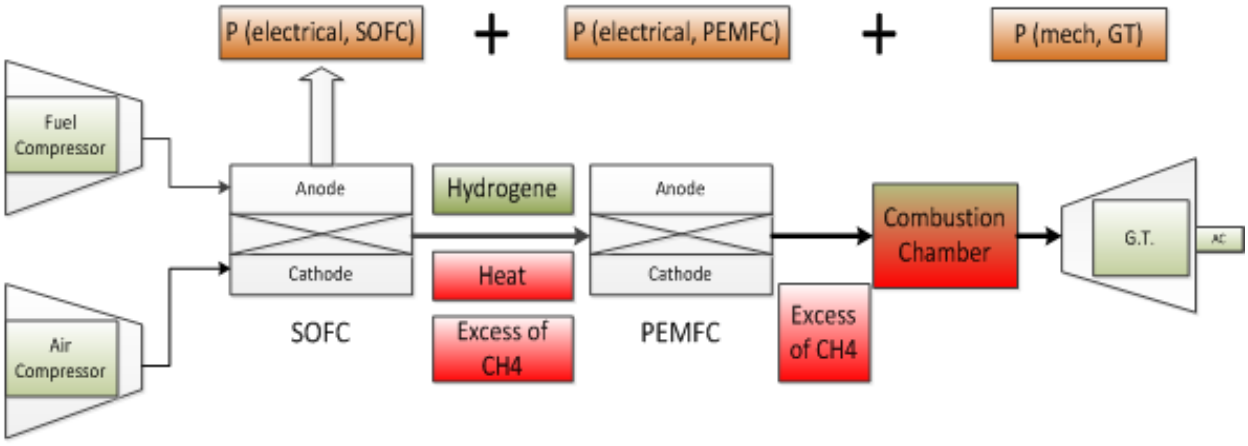

Figure 3: Schematic diagram of the proposed integrated system

In addition to this, the hot air leaving the anode of the PEMFC is routed to a combustor to heat the air to raise its temperature before entering the gas turbine to maximize the turbine efficiency. However, as the turbine is a mass-flow device, combining the steam with the high-temperature gases will increase the total electrical power produced. Furthermore, another important advantage is that the water contents of the gas mixture entering the turbine decreases the temperature in the interior of the turbine, which permits it to gain more efficiency via increasing the temperature of the fuel combustion.

1.8 SOFC Model

The SOFC fuel can be methane, natural gas, or hydrogen. However, in this study, natural gas is being used as a fuel in order to make use of the hydrogen which will be produced from the chemical reactions inside the SOFC. The produced hydrogen will be then used as the fuel for the PEMFC. To be able to sustain the reforming and shift reaction of the SOFC stack within the anode compartment, we need to operate in the usual operating temperature of 800-1100 C.

An internal reforming arrangement also provides additional cooling of the stack because part of the heat released by the electrochemical reaction is used internally by the methane reforming reaction. The chemical reactions include the methane reforming process and the water gas-shift reaction in the shift reactor as follows: [4]

Steam Reforming: $CH_4 + H_2O \rightarrow CO + 3H_2$ (1)

Shift Reactor: $CO + H_2O \rightarrow CO_2 + H_2$ (2)

where in the steam reforming process both CO and hydrogen will be produced and then directed to the shift reactor where more hydrogen is produced before the flow stream enters the PEMFC.

Figure 4 below shows a detailed energy balance diagram of the SOFC stack.

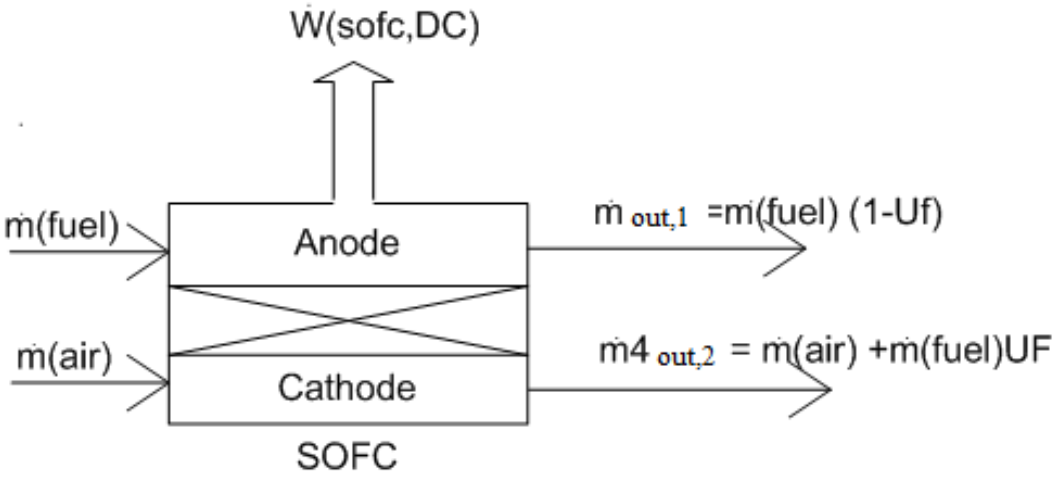

Figure 4: SOFC Model

1.8.1 PEMFC Model

The PEMFC model represents a particular fuel cell stack where the parameters such as pressures, temperature, compositions, and flow rates of fuel and air vary. These variations affect the open circuit voltage as well as the Tafel slope. The open circuit voltage, E_{OC}, and the Tafel slope, A, are modified as follows [8]:

$$E_{OC} = N(E_n - A\ln(i_0)) \tag{3}$$

and:

$$A = \frac{RT}{z\alpha F} \tag{4}$$

where:

R = 8.3145 J/(mol K)

F = 96485 A s/mol

The rate of conversions (utilizations) of hydrogen, $U_{f,H2}$, and oxygen, $U_{f,O2}$, are determined in Block A as follows:

$$U_{f,H2} = \frac{60000RTNi_{fc}}{zFP_{Fuel}V_{lpm(fuel)} \times x\%} \quad 0 \leq U_{f,H2} < 1 \tag{5}$$

and:

$$U_{f,O2} = \frac{60000RTNi_{fc}}{zFP_{air}V_{lpm(air)} \times y\%} \quad 0 \leq U_{f,O2} < 1 \tag{6}$$

1.8.1.1 PEMFC Mass Balance

The fuel mass flow rate can be determined using the following equation:

$$m_{H2,in} = \frac{1}{U_{f,H2}} \frac{M_{H2}}{2F} I.n_{cell} \quad (7)$$

similarly the oxygen flow rate is obtained as follows:

$$m_{O2,in} = \frac{1}{U_{f,O2}} \frac{M_{O2}}{2F} I.n_{cell} \quad (8)$$

and the air mass flow rate is:

$$m_{air,in} = \frac{r_{O2}}{U_{f,O2}} \frac{M_{air}}{2F} I.n_{cell} \quad (9)$$

Finally, the flow rate of the air leaving the cathode of the PEMFC stack is calculated as follows:

$$m_{air,out} = [\left(\frac{1}{U_{f,O2}} - 1\right) M_{O2} + \frac{1}{U_{f,O2}} \frac{1 - r_{O2,in}}{r_{O2,in}} M_{N2}] \frac{I.n_{cell}}{4F} \quad (10)$$

Figure 5 below shows a detailed energy balance diagram of the PEMFC stack [5].

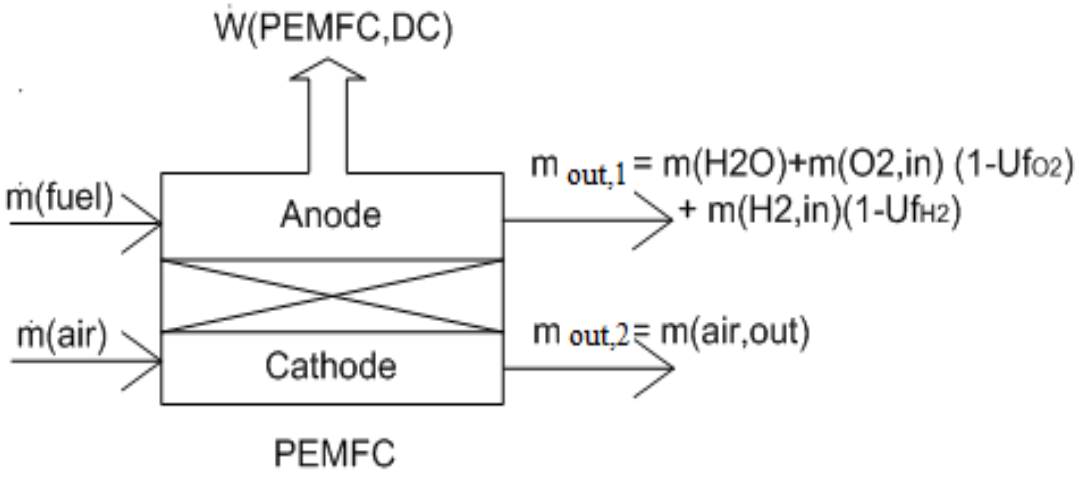

Figure 5: PEMFC Model

1.8.1.2 PEMFC Model Assumptions

The assumptions held when designing the PEMFC model are as follows [9]:

- The gases are ideal.
- The stack is fed with hydrogen and air.
- The stack is equipped with a cooling system that maintains the temperature at the cathode and anode exits stable and equal to the stack temperature.

- The stack is equipped with a water management system to maintain the humidity inside the cell at an appropriate level at any load.
- For output current less than 1 A, the output voltage is closed to the open circuit voltage.

1.8.1.3 PEMFC Model Limitations

The limitations of the PEMFC model are as follows:

- Chemical reaction dynamics caused by partial pressure changes of chemical species inside the cell are not considered.
- The stack output power is limited by the fuel and air flow rates supplied.
- The effect of temperature and humidity of the membrane on the internal resistance is not considered.

1.8.2 Modelling of the Compressors, Turbine, and Combustor

1.8.2.1 Compressor

In the proposed system, two compressors are being used. One is the air compressor, and the other one is the fuel compressor. Both compressors should have the same pressure ratio, which means that they should have same operating pressures and temperatures. The equations below describe the model of the air compressor; however, the same equations are applied to simulate the fuel compressor. [2]

The isentropic efficiency of the air compressor is defined as:

$$\eta_c = \frac{W_{cs}}{W_{ca}} = \frac{h_{2s} - h_1}{h_2 - h_1} \tag{11}$$

The ideal temperature of the working fluid (air) at the compressor outlet can be determined from the following equation:

$$\frac{T_{2s}}{T_1} = \left(\frac{P_2}{P1}\right)^{\frac{(\gamma-1)}{\gamma}} \tag{12}$$

Work done in both the air compressor and the fuel to produce a pressure ratio of rp are calculated as follows:

$$\eta_c = \frac{W_{cs}}{W_{ca}} = \frac{h_{2s} - h_1}{h_2 - h_1} \tag{13}$$

$$\dot{W}_c = \dot{m}_{air}(h_2 - h_1) + \dot{m}_{fuel}(h_{15} - h_{14}) \quad (14)$$

The entropy generation during the total compression process is calculated as follows:

$$\dot{S}_{gen,c} = \dot{m}_{air}(s_2 - s_1) + \dot{m}_{fuel}(s_{15} - s_{14}) \quad (15)$$

1.8.2.2 Gas Turbine

In the proposed model, the gas turbine has two main functions which are to produce electricity, and to run the compressors.

The isentropic efficiency of the air compressor is defined as: [2]

$$\eta_c = \frac{W_{GTa}}{W_{GTs}} = \frac{h_{\text{before Turbine}} - h_{\text{actual turbine}}}{h_{\text{before Turbine}} - h_{s,\text{turbine}}} \quad (16)$$

The ideal temperature of the working fluid (air) at the outlet of the GT can be determined from the following equation:

$$\frac{T_{\text{Turbine Outlet,s}}}{T_{\text{Turbine Outlet}}} = \left(\frac{P_{\text{Turbine Outlet}}}{P_{\text{Turbine Inlet}}}\right)^{\frac{(\gamma-1)}{\gamma}} \quad (17)$$

The total amount of work transmitted generated can be calculated as follows [26]:

$$\dot{W}_{GT} = \dot{m}_5(h_5 - h_6) \quad (18)$$

The entropy generation during the total expansion process can be calculated as:

$$\dot{S}_{gen,c} = \dot{m}_5(s_6 - s_5) \quad (19)$$

1.8.2.3 Combustor

The pressurized flow leaving the anode of the PEMFC stack is being heated in the combustor before it is mixed with the flow leaving the cathode of the SOFC stack. The equation for calculating …. is as follows:

$$\dot{m}_{12} + \dot{m}_{fuel,comb} = \dot{m}_{13} \quad (20)$$

In addition, the combustor energy balance can be expressed as:

$$\dot{m}_3 h_3 + \dot{Q}_{comb} - \dot{m}_{13} h_{13} - \dot{Q}_{loss} = 0 \quad (21)$$

Where the heat generated in the combustor is:

$$\dot{Q}_{comb} = (\dot{m}_3 + \dot{m}_{Fuel,Comb}) \times LHV \quad (22)$$

And the heart loss in the combustor is:

$$\dot{Q}_{loss} = \dot{Q}_{comb}(1 - \eta_{comb}) \quad (23)$$

Finally, the entropy generation within the combustor can be calculated as follows:

$$\dot{S}_{gen,comb} = \dot{m}_{13}s_{13} - \dot{m}_{12}s_{12} - \dot{m}_{fuel,comb}s_{fuel,comb} + \frac{\dot{Q}_{loss}}{T_{surr}} - \frac{\dot{Q}_{Comb}}{T_{comb}} \quad (24)$$

1.8.3 Overall Balance Equations For The Integrated Cycle

The integrated gas turbine power plant may be analyzed as one control volume as shown schematically in Figure 6, which shows the inlet and outlet flows (including mass flow, heat, and work) at the boundary of the system.

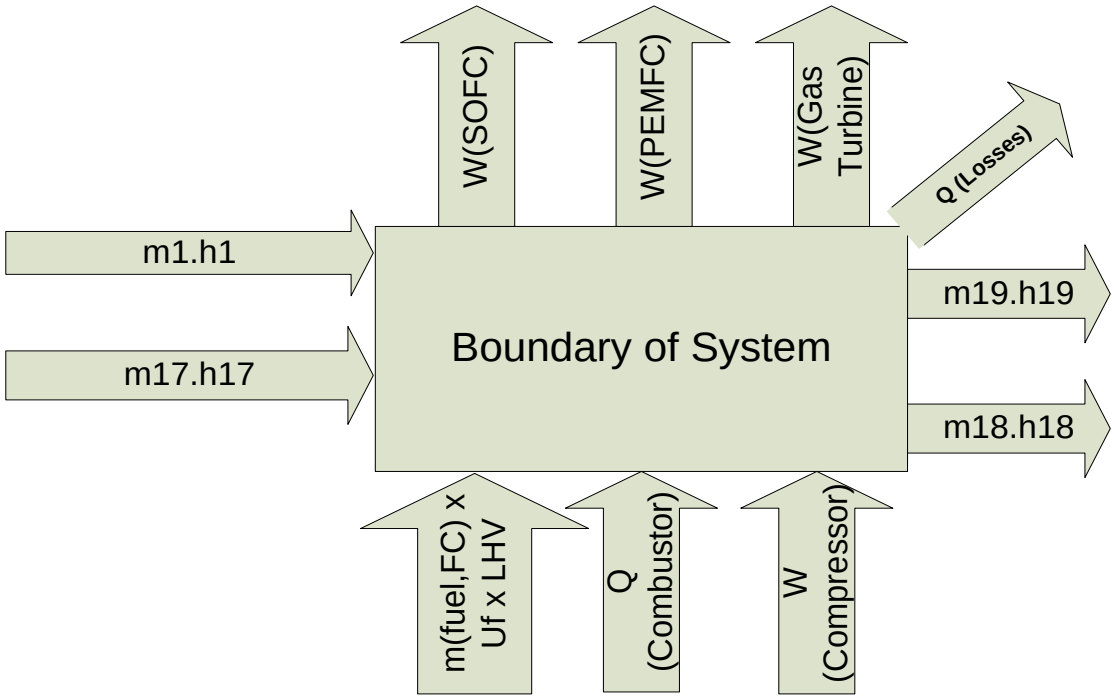

Figure 6: Energy balance for the overall system

Chapter 2: Technical and Economic Analysis of Fuel Cells

2.1 PEMFC and SOFC Simulation

2.1.1 SOFC Operating Conditions

The SOFC simulation was done using MATLAB Simulink, where the following parameters (shown in Table 1) were assumed to be fixed: [9]

Table 1: SOFC Simulation parameters

Setting Parameter	Value
Environment pressure (bar)	1
Environment temperature (°C)	25
Fuel utilization factor	0.85
Minimum steam-to-carbon ratio	2
Cell current density (mA/cm^2)	100
Anode thickness (cm)	0.0010
Cathode thickness (cm)	0.19
Interconnection thickness (cm)	0.0094
Anode activation energy (kJ/kmol)	1.1×10^5

2.1.2 SOFC Simulation

The performance of a fuel cell stack is usually described by plotting the well-known polarization curve, which relates the cell voltage to its current density. This plot is affected by all the typical losses of the fuel cell under investigation and can be used to analyze their values. The polarization curve of the SOFC used in the stack of this study is represented in Figures 7 and 8 below.

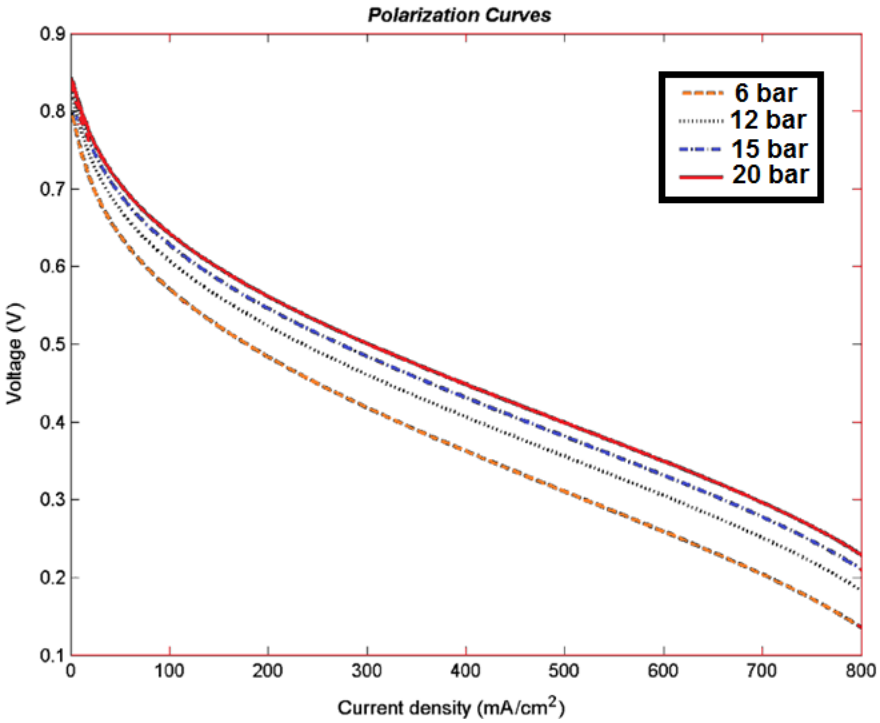

Figure 7: SOFC Stack Polarization Curve at a Temperature of 750 C

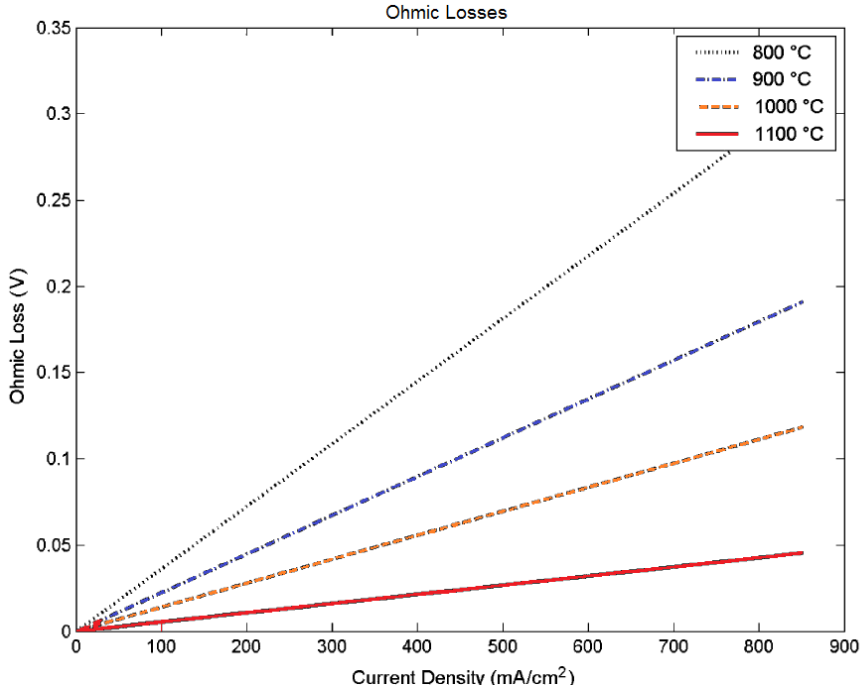

Figure 8: SOFC Stack Ohmic Losses Curve at a pressure of 20 bar

Figure 8 shows the dependence of the SOFC voltage on the operating temperature. In order to plot these figures other important parameters such as the total pressure, water, hydrogen and oxygen partial pressures are also considered. According to the Nernst equation, it can be observed that the cell voltage value increases by raising the operating pressure, hydrogen, and oxygen partial pressures, or by lowering the anode water molar fraction. From the achieved results, it can also be observed that by increasing p_{H2} and p_{O2}, lower values of fuel and air utilization factors are achieved. Moreover, by increasing cell operating pressure, it is possible to gain best performance even if a higher cost must be taken into account, due to the energy and investment for compressors. The Ohmic, concentration, and activation losses decide the shape of the SOFC polarization curve. The Ohmic losses in the SOFC are due to interconnections among anode, cathode, and electrolyte. In order to reduce the losses and the overvoltage, the cell thickness should be reduced and the operating temperature should increase. In this simulation, the concentration overvoltage is taken into account by using a simplified approach based on Fick's law. In this simulation, Fick's Law is applied to simplify the approach to take into account the concentration overvoltage. Accordingly, the limiting current density value is considered a fixed parameter.

2.1.3 PEMFC Simulation

A 30 kW fuel cell stack model was constructed and then simulated using MATLAB. The simulated PEMFC compromises a total of 500 cells. The cells' fixed parameters are assumed to be as follows: [8]

- Stack Open Circuit Voltage: 490 V
- Nominal Voltage: 340 V
- Nominal Operating Current: 50 A
- Cathode Supply Air Pressure: 1 bar
- Cathode Supply Air Flow Rate: 4500 Lpm

The PEMFC simulation was studied at different operating fuel pressures and temperatures. The pressure levels were varied from 10-20 bar to simulate the effect of changing the pressure ratio for the cycle. Furthermore, the temperature values were varied from 370 K to 440 K.

Figure 9 below shows the Simulink model used to simulate the performance of the PEMFC.

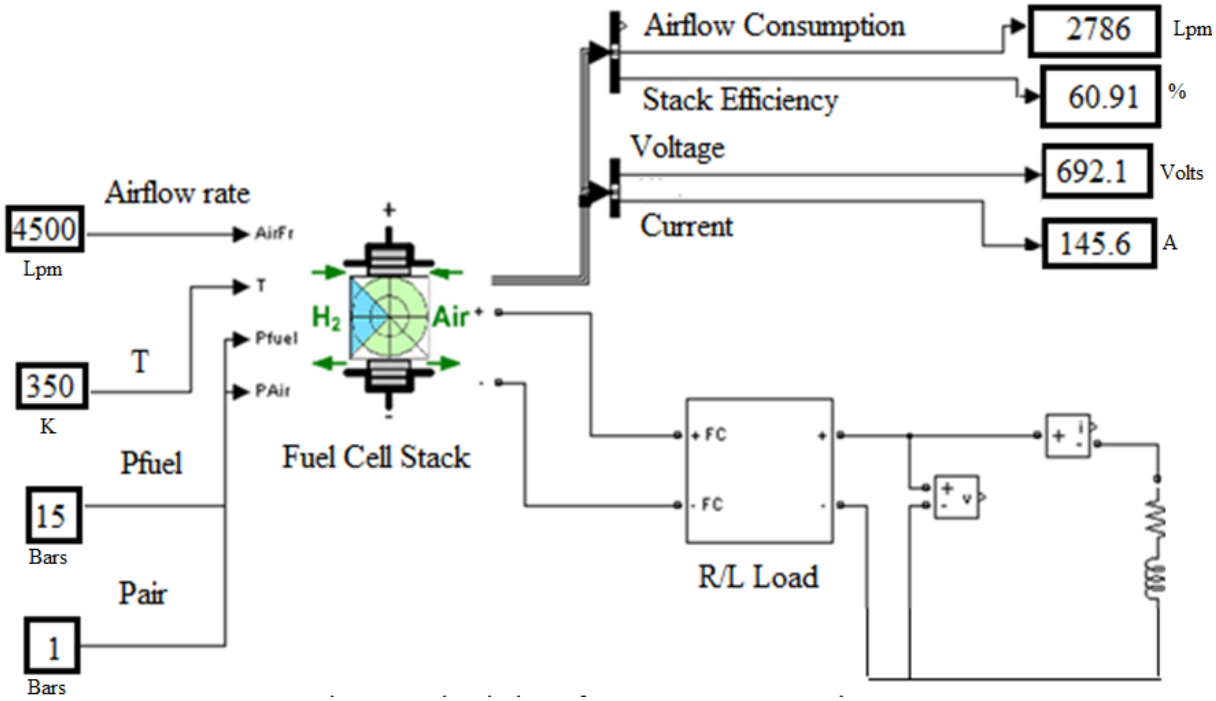

Figure 9: Simulation of 30 kW PEMFC Stack

Based on the simulation results, several plots of fuel cell stack polarization curves at different operating pressures and temperatures are shown in Figures 10 and 11.

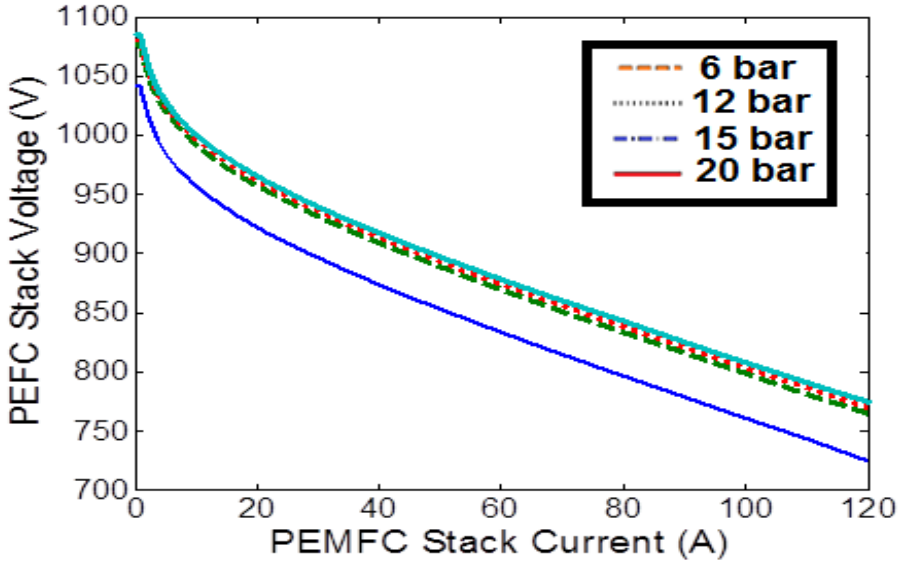

Figure 10: PEMFC Stack efficiency at different operating fuel pressure and at a temperature of 42

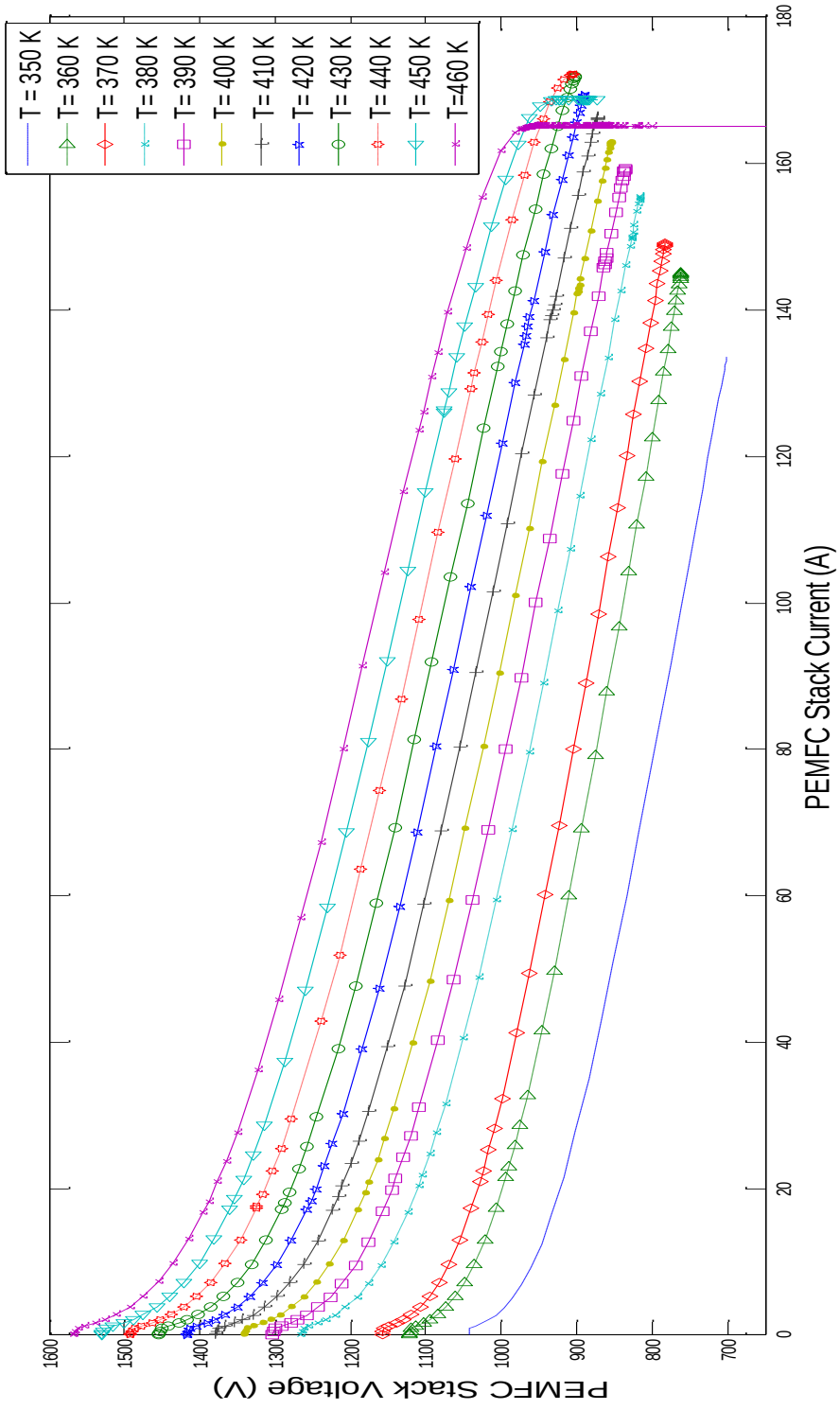

Figure 11: PEMFC Stack polarization curve at different operating temperatures and at a fuel pressure of 20 bar

Table 2 below shows the results of efficiency and power obtained at different operating fuel pressures and temperatures.

Table 2: Simulation Results of PEMFC Stack

Fuel Pressure (bar)	Stack Temperature (K)	Efficiency (%)	Current (A)	Voltage (Volts)	Power (W)
10	375	59.8%	57.2	453.33	25,930.67
10	400	69.9%	66.8	529.47	35,368.37
10	420	70.1%	67.2	531.47	35,714.56
10	440	68.0%	64.88	514.13	33,356.97
15	350	61.0%	58.08	394.73	22,926.11
15	375	71.2%	68.16	540.00	36,806.40
15	400	73.0%	67.6	543.33	36,729.33
15	420	69.0%	65.2	514.00	33,512.80
20	350	62.0%	59.2	468.00	27,705.60
20	375	71.0%	69.2	546.67	37,829.33
20	400	74.0%	67.6	533.73	36,080.37
20	420	69.0%	65.2	516.00	33,643.20

Figure 12 below shows the efficiency obtained at different operating fuel pressures and temperatures.

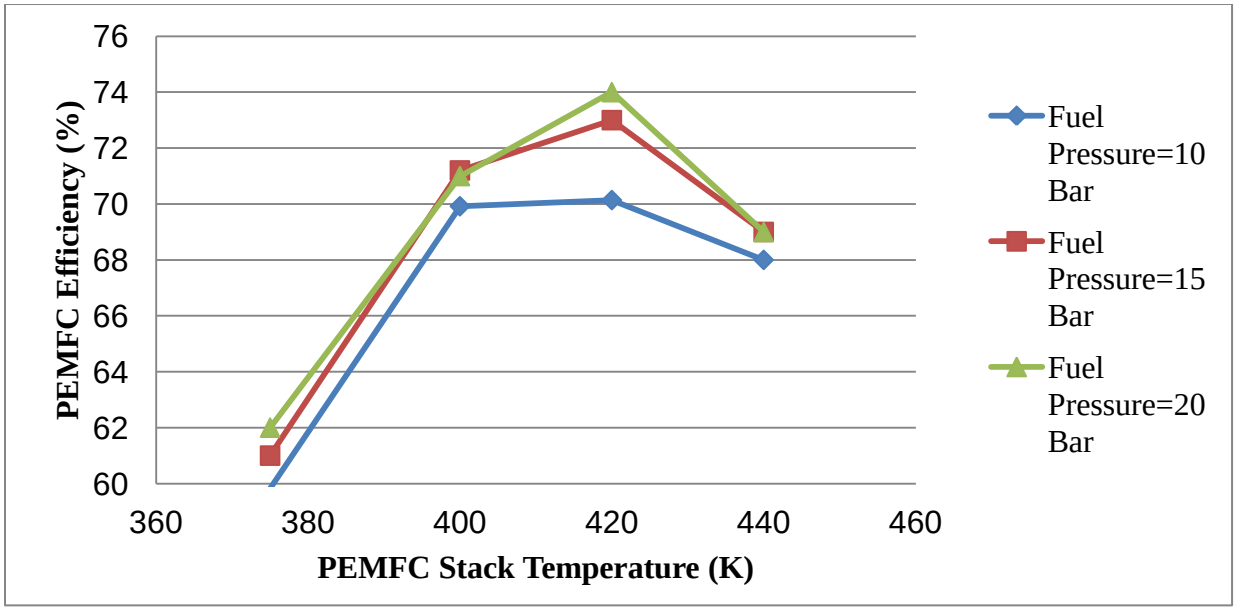

Figure 12: PEMFC Stack efficiency at different stack temperatures and fuel pressures

The results show that by fixing all other parameters and varying the fuel supply pressure and operating temperatures, the PEMFC fuel cell stack efficiency increases as the fuel pressure increases. The PEMFC stack efficiency reached up to 73% at 20 bar and a temperature of 400 K. Furthermore, the total power produced from the PEMFC stack reached up to 37 kW, which is more than 10 kW higher than the nominal expected power at 10 bar and at 375 K.

In addition to this, the results show that at a fuel operating pressure of 20 bar, the PEMFC efficiency increases as temperature increases from 350-420 K until temperature reaches above 420 K where efficiency is maximized, and then the PEMFC starts to operate in an unstable condition. Furthermore, the efficiency also begins to deteriorate when the temperature increases above 440 K.

2.2 Economic Analysis of Fuel Cell Stacks

2.2.1 Methodology

Considering investment, operation, and maintenance, the annual total cost C_t is given by: [13]

$$C_t = C_c + C_f + C_m \quad (25)$$

The annual investment cost C_c is obtained from the total purchasing cost Cfc disregarding the individual cell replacement cost during its lifespan n, as shown in the following equation: [13]

$$C_c = C_{fc}.(i_r(1+i_r)^n)/((1+i_r)^n - 1) \quad (26)$$

where i_r is the annual interest rate (%).

The operation cost C_f depends on the fuel used to produce both the electric energy E_{ep} and the thermal energy E_{th}.

Considering Eth as a by-product (with fixed E_{ep}=E_{th} ratio), the production cost can be expressed as:

$$C_f = (\gamma_{ng}.E_{ep})/\eta \quad (27)$$

Where γ_{ng} is the price of natural gas ($/kWh) and η is the electrical efficiency (%).

The maintenance cost C_m depends on the technology used, but it can be expressed as a percentage of the purchasing cost (4–10%).

The unit cost γ_P of produced energy ($/kWh) can be obtained from the annual production E_p:

$$\gamma_P = C_t/E_P \quad (28)$$

Likewise, the produced electric energy can be sold to th. In the physical form, the thermal energy and the electrical energy can be treated equally and may be expressed in terms of kWh:

$$E_p = E_{es} + E_{th} \quad (29)$$

It is assumed that the extra electricity can be sold with special price Ges while the extra thermal energy can't be sold but can be utilized in different applications.

The economic value between thermal energy and electrical energy cannot be treated equally as they are priced differently in the market. Assuming a constant production, the yearly benefit B is simply

$$B = E_{es}(\gamma_{es} - \gamma_p) + E_{th}(\gamma_{th}) \quad (30)$$

where γ_{es}, γ_{ec} and γ_{th} are, respectively, the electricity selling price, the electricity buying price, and the thermal buying price ($/kWh).

The net present value (NPV) and internal rate of return (IRR) are the two financial metrics used for economic feasibility analysis.

The NPV is equal to the present value of the future cash flows returned by a project, minus the initial investment.

$$NPV = (\sum_{t=1}^{n} \frac{B}{(1+i_r)^t}) \quad (31)$$

The criteria for acceptance for the NPV are straightforward: the project will be accepted only if its NPV is greater than zero.

The IRR is the value of the discount rate 'd' at which make the NPV value equal to zero. Its calculation is done by

$$NPV_{d=IRR} = 0 \quad (32)$$

NPV can be interpreted as some kind of income the owner of the SOFC generator can get during the whole life span of the SOFC, discounted by an interested rate.

IRR means the interest rate the user can get from the SOFC generation investment. Accordingly, if this interest rate is higher than that of the bank, the opportunity cost of

SOFC investment is higher than that of deposit in the bank, making the latter choice economically infeasible when a householder has extra capital.

2.2.2 Life time of Fuel Cells

The typical PEMFC lifetime in stationary applications may reach 30,000 hours which is around 4 years. SOFC typical lifetimes are around of 40,000-60,000 hours which is around 5-6 years. For this thesis the lifetime of the SOFC stack is assumed to be 5 years.

2.2.3 SOFC Calculations and Sensitivity Analysis

The analysis of the SOFC was done based on the equations mentioned in the previous section, and is based on the following assumptions:

1. The SOFC stack consists of 1000 cells
2. The rated power of the SOFC stack is 130 kW
3. The fuel supplied to the SOFC is coming from the fuel compressor at a pressure of 20 bar

Table 3 below shows the parameters used to perform the feasibility study on the SOFC.

Table 3: SOFC Economic Analysis Parameters

Input	Value
C_{fc} ($)	$55,000
C_c ($)	$18,478
C_f ($)	$125,268
C_m ($)	$8,000
y_{ng} ($/kWh)	0.065
y_p ($/kWh)	0.096
yth ($/kWh)	0.05
y_{es} ($/kWh)	0.16
i_r	5%
Pe (kW)	110
Pth (kW)	70
E_{es} (kWh)	963,600
E_{th} (kWh)	613,200
n (years)	5

In order to perform a successful sensitivity analysis on the SOFC stack, it is required to identify all the possible sources of risk and then study their effect on the NPV of the system under study. Below are the five major risk factors identified for the study of the economic feasibility of the SOFC and PEMFC stacks.

1. Improvements in the electrical efficiency

The economic feasibility of an SOFC is very sensitive to the efficiency, which is determined by the technology development and/or the internal design of the SOFC. Of course, the NPV will increase with increasing efficiency and decreasing purchasing cost (Cfc).

Table 4 below shows the NPV values obtained at different fuel cell efficiencies in addition to the percentage error comparing with the NPV at standard efficiency.

Table 4: Sensitivity Analysis based on changes in Fuel Cell Efficiency

Fuel Cell Efficiency (%)	**NPV (USD)**	**Error in Value (%)**	**Error in NPV (%)**
40%	($47,323.84)	-20.00%	-153.62%
45%	$28,001.84	-10.00%	-68.27%
50%	$88,262.38	0.00%	0.00%
55%	$137,566.46	10.00%	55.86%
60%	$178,653.20	20.00%	102.41%

2. Changes in the Electricity Prices

In order for governments to support the investment in fuel cell systems, the governments tend to provide favorable tariffs, or premium prices to purchase electricity produced from SOFC due to the fact that it is environmental friendly. In a theoretical framework, this evaluates the impact of strength of the government policy in a premium price range ($\gamma_{es} = 0.14 - 0.18$ \$/kWH) [25].

Table 5 below shows the Net Present Value (NPV) obtained after varying the electricity prices from $0.14 to $0.18.

Table 5: Sensitivity Analysis based on Changes in Electricity Prices

Electricity Price (USD)	NPV	Error in Value	Error in NPV
$0.14	$4,824.71	-12.50%	-94.53%
$0.15	$46,543.55	-6.25%	-47.27%
$0.16	$88,262.38	0.00%	0.00%
$0.17	$129,981.22	6.25%	47.27%
$0.18	$171,700.06	12.50%	94.53%

3. Changes in Initial investment cost

Table 6 below shows the NPV values at different initial investment costs. As mentioned earlier, the estimated cost for the fuel cell stack is $55,000, and the analysis was done by varying the initial cost from $45,000 to $65,000.

Table 6: Sensitivity Analysis based on changes in the Capital Cost

Initial Investment (USD)	NPV	Error in Value	Error in NPV
$45,000	$98,262.38	-18.18%	11.33%
$50,000	$93,262.38	-9.09%	5.66%
$55,000	$88,262.38	0.00%	0.00%
$60,000	$83,262.38	9.09%	-5.66%
$65,000	$78,262.38	18.18%	-11.33%

4. Changes in Interest Rate

Table 7 below demonstrates the effect of changing the interest rates on the NPV value. The interest rate was varied from 1% (best case scenario) and 9% (worst case scenario).

Table 7: Sensitivity Analysis based on changes on the interest rate

Interest Rate	NPV	Error in Value	Error in NPV
1%	$105,600.04	80.00%	19.64%
3%	$96,542.51	40.00%	9.38%
5%	$88,262.38	0.00%	0.00%
7%	$80,675.53	-40.00%	-8.60%
9%	$73,708.56	-80.00%	-16.49%

5. Changes in Electrical Power Produced

Table 8 below shows the sensitivity analysis results after varying the total electrical power produced from the SOFC stack.

Table 8: Sensitivity Analysis based on changes in electrical power produced

Electric Power Produced (kW)	NPV (USD)	Error in Value (%)	Error in NPV (%)
90	$65,506.65	-18.18%	-25.78%
100	$76,884.52	-9.09%	-12.89%
110	$88,262.38	0.00%	0.00%
120	$99,640.25	9.09%	12.89%
130	$111,018.11	18.18%	25.78%

Figure 13 below shows the spider plot based on the results obtained after performing sensitivity analysis on the SOFC stack after identifying all the possible sources of risk.

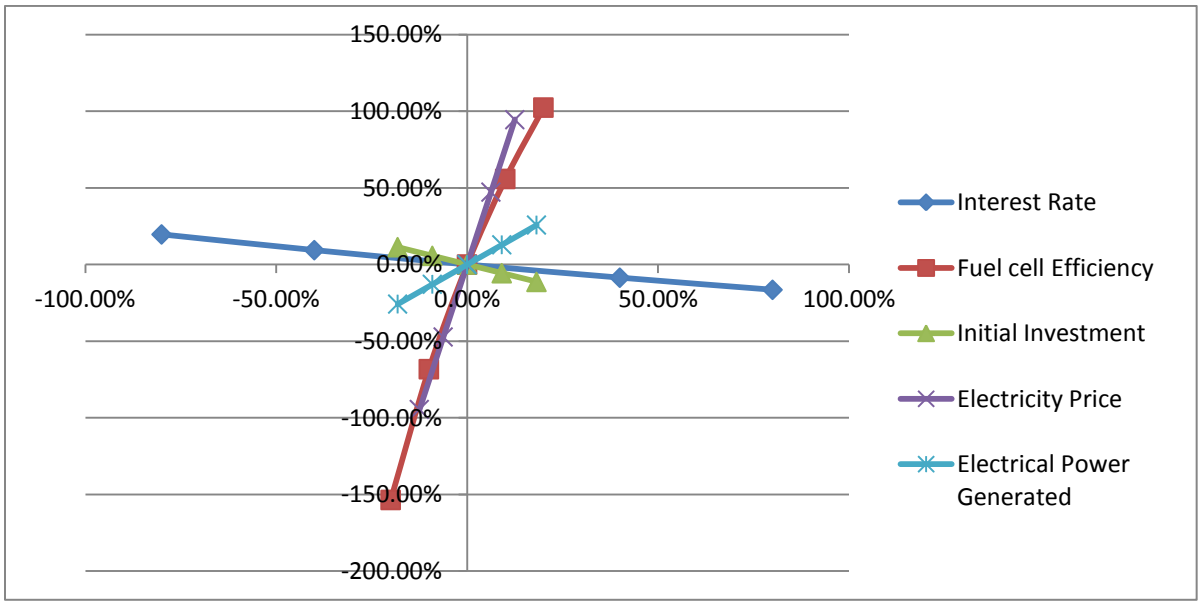

Figure 13: Spider plot for SOFC

Based on the sensitivity analysis, the most two critical factors which affect the SOFC investment are the fuel cell efficiency and electricity price. Since these two factors may result in a negative NPV, they can be considered as possible risks.

2.2.4 PEMFC Calculations and Sensitivity Analysis

The analysis of the PEMFC was done based on the equations mentioned in the previous section, and is based on the following assumptions:

1. The PEMFC stack consists of 500 cells.
2. The rated power of the PEMFC stack is 40 kW.
3. The hydrogen which is used as a fuel for the PEMFC is generated in the chemical reactions of the SOFC so there is no cost for the fuel.
4. The lifetime of the PEMFC is 4 years.

Table 9 below shows the economic parameters and the assumed costs required to perform the sensitivity analysis for the PEMFC stack.

Table 9: Economic parameters and estimated costs to perform sensitivity analysis

Input	**Value (USD)**
C_{fc} ($)	$25,000
Cost of Water for Cooling	$2,000
C_m ($)	$4,000
y_{es} ($/kWh)	0.17
i_r	5%
Pe (kW)	30
E_{es} (kWh)	262,800
n (years)	4

Similar to the SOFC, the sensitivity analysis of the PEMFC stack was done on the same risk factors identified.

1. Changes in the Electricity Prices

Table 10 below shows the NPV values obtained after varying the electricity prices from $0.14 to $0.18.

Table 10: Sensitivity analysis based on changes of electricity prices

Electricity Price	NPV	Error in Value	Error in NPV
0.14	$98,313.25	-12.50%	-18.80%
0.15	$109,691.11	-6.25%	-9.40%
0.16	$121,068.98	0.00%	0.00%
0.17	$132,446.84	6.25%	9.40%
0.18	$143,824.70	12.50%	18.80%

2. Changes in Initial Investment Cost

An internal analysis of the fuel cell manufacturing costs conducted at Energy Partners indicated that the cost of fuel cells could be reduced by 10 times if mass production techniques (i.e. ten thousand 10 kW units per year) were applied in the manufacturing process, including manufacturing of membranes and electrodes. This would result in about $50 per cell plus $150 per stack. This is still a more conservative estimate than the Allison Gas Turbine Division's findings that the cost of a fuel cell for automotive applications should be as low as $30/kW.

Table 11 below shows the NPV values at different initial investment costs. As mentioned earlier, the estimated cost for the PEMFC stack is $35,000, and the analysis was done by varying the initial cost from $25,000 to $45,000.

Table 11: Sensitivity analysis based on changes of initial investment cost

Initial Investment	NPV	Error in Value	Error in NPV
25000	$131,068.98	-28.57%	8.26%
30000	$126,068.98	-14.29%	4.13%
35000	$121,068.98	0.00%	0.00%
40000	$116,068.98	14.29%	-4.13%
45000	$111,068.98	28.57%	-8.26%

3. Changes in Interest Rate

Table 12 below demonstrates the effect of changing the interest rates on the NPV value. The interest rate was varied from 1% (best case) and 9% (worst case).

Table 12: Sensitivity analysis based on changes of interest rate

Interest Rate	NPV	Error in Value	Error in NPV
1%	$139,956.49	-80.00%	15.60%
3%	$130,089.28	-40.00%	7.45%
5%	$121,068.98	0.00%	0.00%
7%	$112,803.92	40.00%	-6.83%
9%	$105,214.15	80.00%	-13.10%

4. Changes in Electrical Power Produced

Table 13 below shows the sensitivity analysis results after varying the total electrical power produced from the PEMFC stack.

Table 13: Sensitivity analysis based on changes of electrical power produced

Electric Power Produced	NPV	Error in Value	Error in NPV
20	$60,387.03	-33.33%	-50.12%
25	$90,728.00	-16.67%	-25.06%
30	$121,068.98	0.00%	0.00%
35	$151,409.95	16.67%	25.06%
40	$181,750.92	33.33%	50.12%

Figure 14 below shows the spider plot based on the results obtained after performing a sensitivity analysis on the PEMFC stack for all the possible sources of risk.

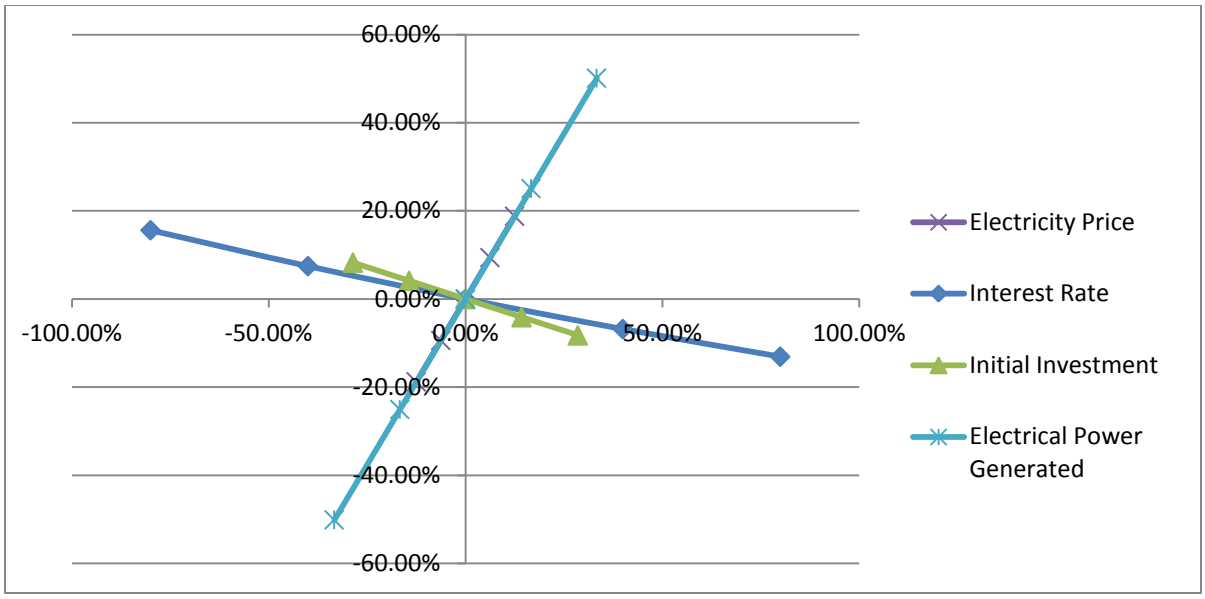

Figure 14: PEMFC Spider Plot

As shown in Figure 14, the most critical two factors which affect the NPV from the PEMFC are the electricity price and the electrical power generated from the PEMFC. However, since none of the two factors may generate a negative NPV, the risk is minimal.

Chapter 3: Comparative Analysis Between Conventional And Fuel Cell Based Gas Turbine Power Plants

3.1 Layouts of the Systems under Study

Figures 15, 16, and 17 below show the three systems which are under study in this paper and which will be compared technically and economically.

The first system which is shown in Figure 15 below is the conventional gas turbine system with two compressors, a combustion chamber, and the gas turbine.

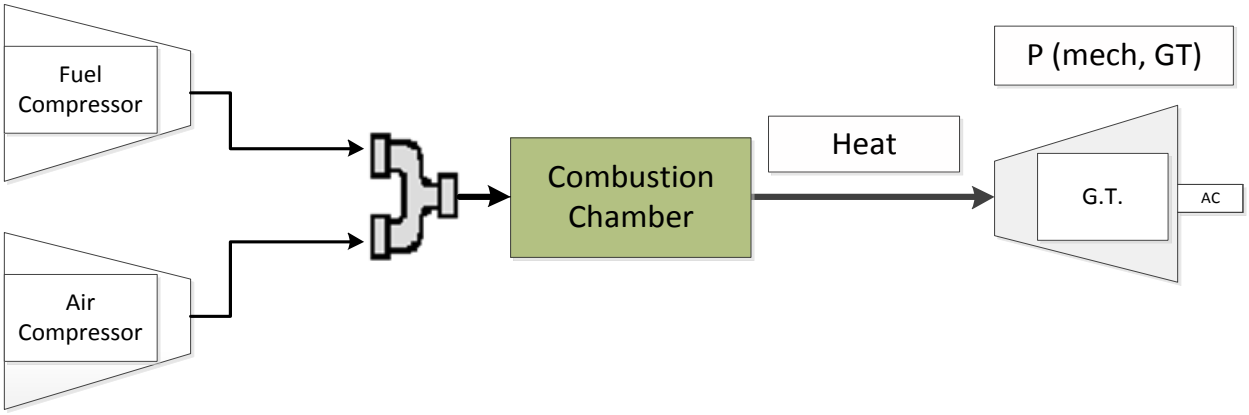

Figure 15: Layout of the Conventional Gas Turbine Integrated System

The second system to be evaluated is the SOFC integrated into the gas turbine cycle. The main advantage of integrating the SOFC into the cycle is to pre-heat the compressed mixture of fuel and gas before entering the combustion chamber to save energy, and to also generate additional electrical energy from the reactions in the SOFC. Figure 16 below shows the proposed system:

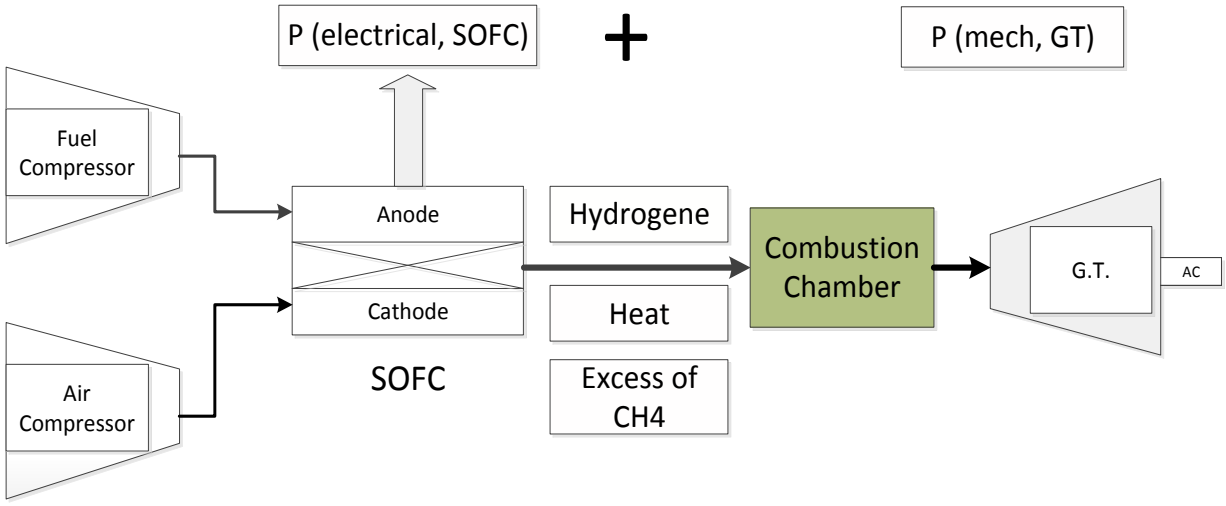

Figure 16: Layout of SOFC System integrated into Gas Turbine Cycles

Figure 17 below shows the layout of the third system to be evaluated in this paper, where both the PEMFC and the SOFC are integrated into the gas turbine cycle.

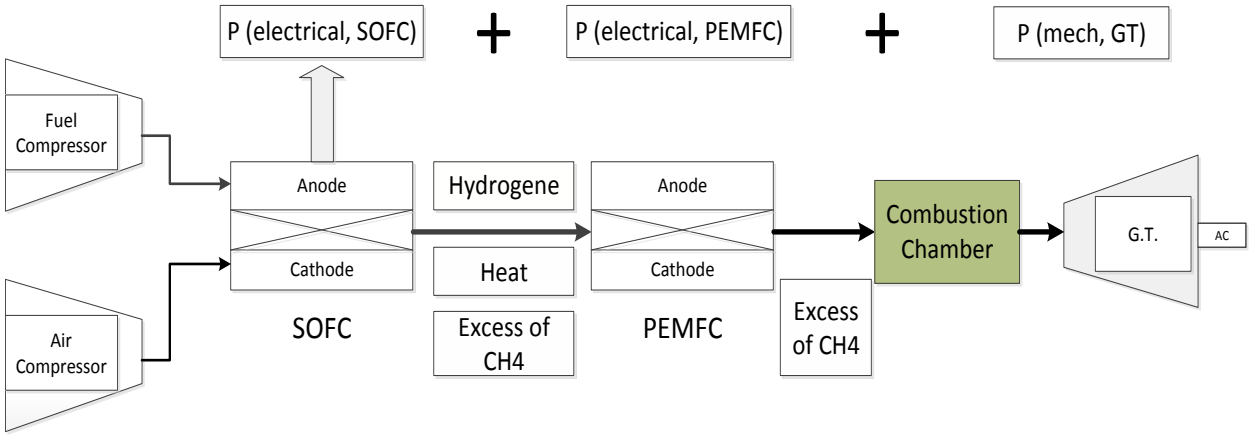

Figure 17: Layout of SOFC & PEMFC System integrated into Gas Turbine Cycles

A simulation of the plant operation was carried out by inserting the governing equations of each component into a MATLAB program, within which a linkage between the cycle compounds was established. The output of a component is treated as the input to the other component located in the downstream direction.

3.2 Operating Characteristics of the proposed Systems

Table 14 below shows the typical operating conditions of a combined SOFC-gas turbine plant. Operating conditions for a PEMFC stack were previously shown [7].

The ISO Operating Temperature is T_0 = 288 K, and P_0 = 1 atm. [8]

Table 14: Main Operating Parameters of the PEMFC+SOFC-GT Plant

Compressor efficiency	0.81
Turbine efficiency	0.84
Combustor Efficiency	0.98
Heat exchanger effectiveness	0.85
Air utilization factor	0.25
Fuel Utilization factor	0.85
LHV CH_4	50,050 kJ/kg
SOFC Stack temperature	750 K
PEMFC Stack Temperature	420 K

3.3 1st Law Analyses of the Proposed Systems

3.3.1 Simulation of the Gas turbine Cycle

In order to investigate the benefits of adding fuel cell systems to the gas turbine cycle, the first step would be to study the performance of the conventional gas turbine cycle under various operating conditions. Figure 18 below shows the Simulink model of the system.

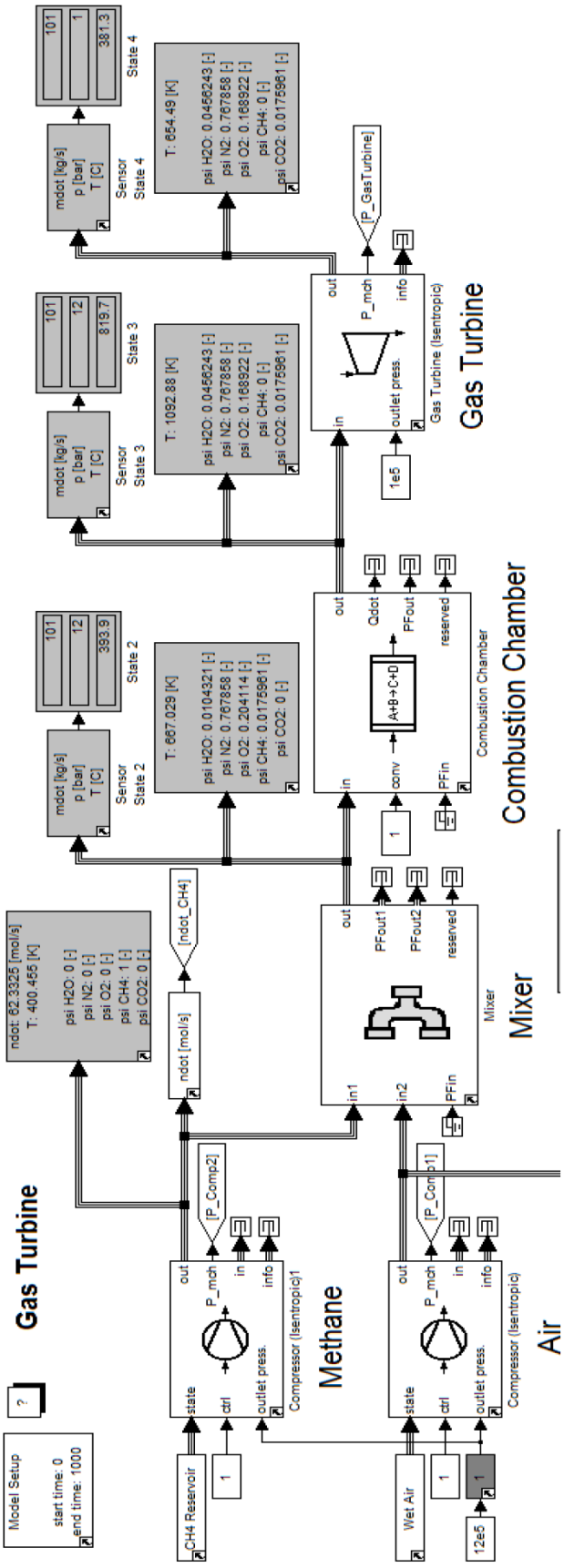

Figure 18: GAS turbine Cycle Layout

As shown in Figure 18, the system consists of two compressors, an air compressor and a fuel compressor, in addition to a mixer where the fuel and the air are mixed before they enter the combustion chamber where the stream is heated before it enters the gas turbine. There are many parameters which decide the efficiency of the system:

1. The flow rate of fuel
2. The flow rate of air
3. The pressure ratio of the compressors
4. The temperature of stream entering the gas turbine
5. The efficiency of the combustion chamber

In order to study the ideal operation conditions, several tests should be implemented to study the cycle efficiency:

3.3.1.1 Factors affect the performance of the cycle

A. Effect of Fuel (Methane) Flow

The first decision variable is the flow rate of fuel required to be supplied to the cycle. This is directly linked to the efficiency of the combustion chamber and the temperature at the turbine inlet. Table 15 below shows the results obtained after varying the fuel flow rate.

Table 15: Turbine power and cycle efficiency based on the changes of the fuel flow

Methane Flow (mol/sec)	**Turbine Power (MW)**	**Cycle Efficiency**
0.62	0.5	35%
1.24	0.75	47%
1.86	0.95	50%
2.5	1.1	51%
3.1	1.2	50.5%
3.75	1.4	48%

Based on the above mentioned results, Figures 19 and 20 show the effect of changing the fuel flow on the thermal efficiency of the cycle and on the turbine power output.

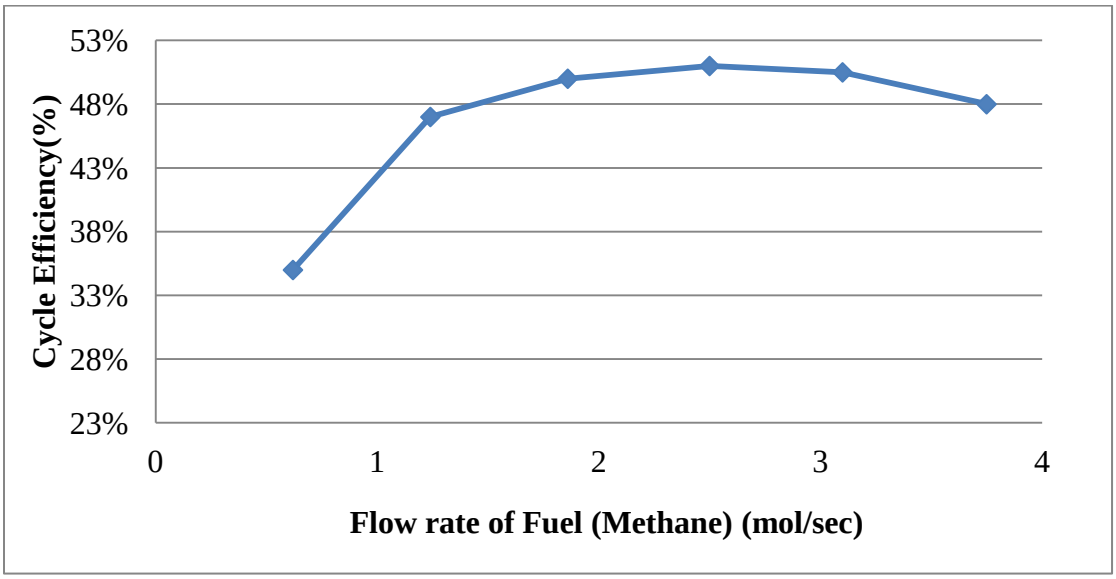

Figure 19: Effect of fuel flow rate on the cycle thermal efficiency at a turbine inlet pressure of 20 bar

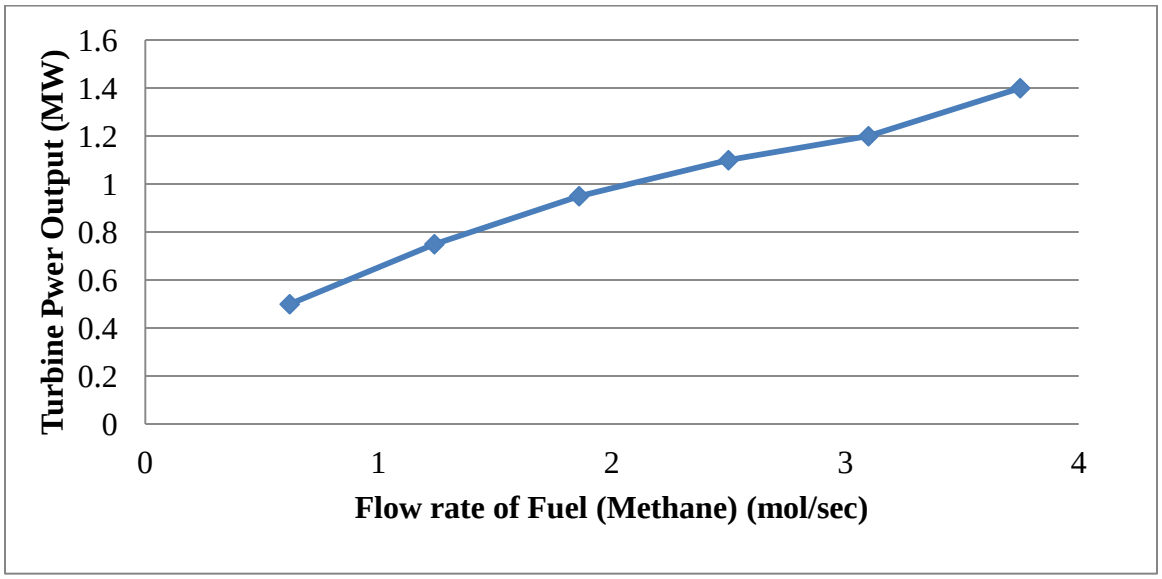

Figure 20: Effect of fuel flow rate on the turbine power output at a turbine inlet pressure of 20 bar

It can be concluded from Figures 19 and 20 that although the turbine power increases with increasing the fuel flow, the turbine efficiency is maximized for a 1 MW cycle when the fuel flow is 2.5 mol/sec.

B. Airflow Rates

Another important decision variable is the airflow rate into the air compressor. Table 16 below shows the turbine power and efficiency at different air flow rates.

Table 16: Turbine power and cycle efficiency based on the changes of the air flow at the inlet

Air Flow (mol/sec)	Turbine Power (MW)	Cycle Efficiency
31	1.1	50.5%
34	1.14	51%
38	1.17	50.5%
42	1.2	50.4%

Figure 21 below shows the relationship between the air flow rate entering the air compressor and cycle efficiency.

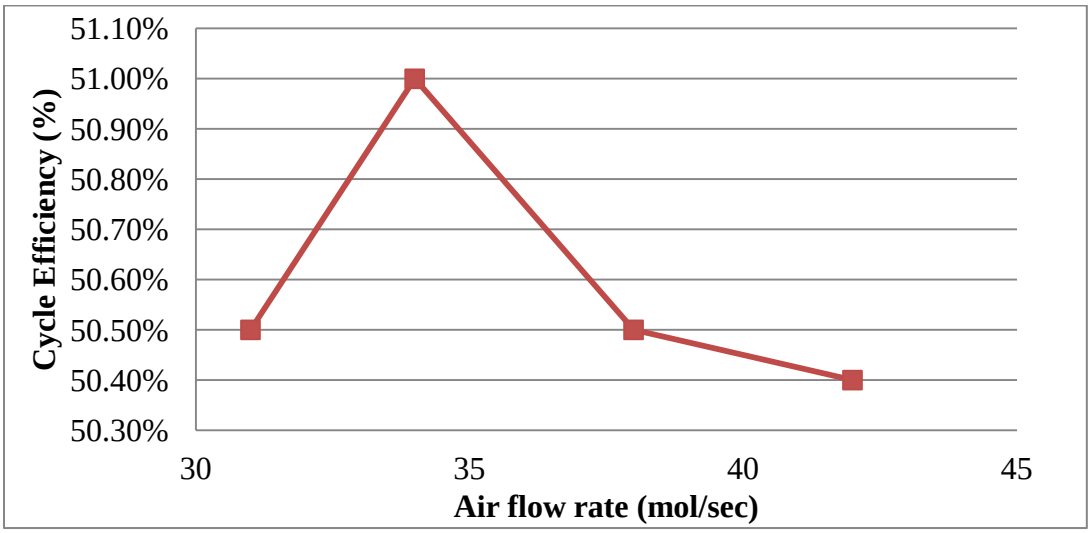

Figure 21: Effect of air flow rate on the cycle thermal efficiency at a turbine inlet pressure of 20 bar and a fuel flow rate of 2.5 mol/sec

As shown in Figure 21, the efficiency is maximized when the airflow rate into the cycle is 34 mol/sec.

C. Compressor Pressure Ratio

Furthermore, one of the most important decision variables which may have a huge effect on the system efficiency is the pressure ratio of both the fuel and air compressors. Table 17 and figure 22 show the output power and efficiency obtained at different pressure ratios and after fixing the fuel flow rate to 2.5 mol/sec and the air flow rate to 34 mol/sec.

Table 17: Turbine power and cycle efficiency

Pressure Ratio	Turbine Power (MW)	Cycle Efficiency (%)
6	0.8	39%
8	0.94	43%
10	1.04	46%
12	1.11	48%
14	1.17	51%
16	1.24	52.5%
18	1.29	54%
20	1.32	54.5%

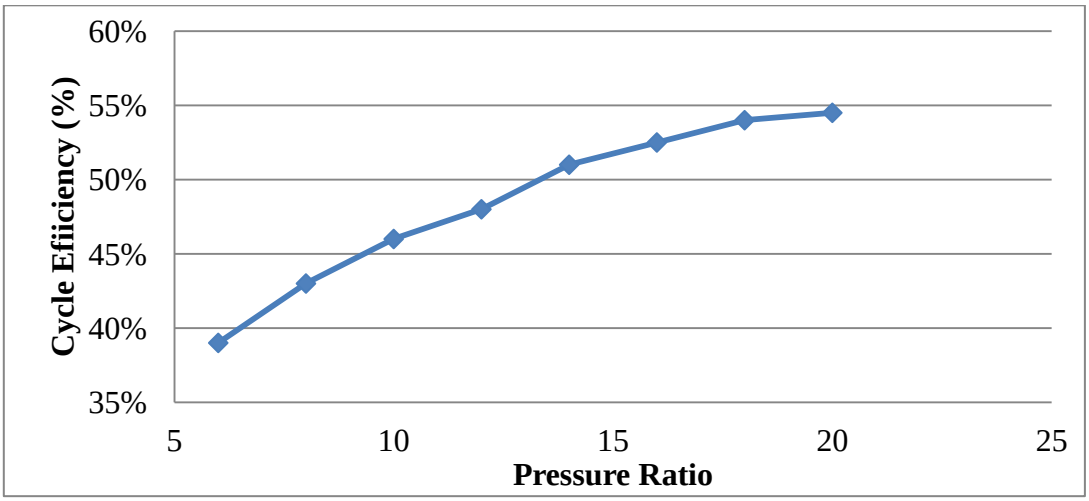

Figure 22: Effect of compressor pressure ratio on the cycle thermal efficiency at an airflow rate of 34 mol/sec and a fuel flow rate of 2.5 mol/sec

Based on the obtained results, the system performance is optimized at a pressure ratio of 20.

3.3.1.2 Thermal Efficiency of the plant

Based on the results, the ideal flow of fuel which results in ideal efficiency is 2.5 mol/sec. Moreover, the ideal airflow rate into the air compressor is 34 mol/sec, and the best results can be obtained at the highest possible pressure ratio for screw compressor which is 20. The efficiency of the gas turbine cycle was then calculated using the following equation:

$$\eta = \frac{P_{mech.GT} - P_{Fuel\ Comp} - P_{Air\ Comp}}{\dot{m}_{fuel} \times LHV_{CH4}} \quad (33)$$

Figure 23 below shows the thermal efficiency calculation for the gas turbine cycle using the Lower Heating Value of CH_4 as 50,050 kJ/kg.

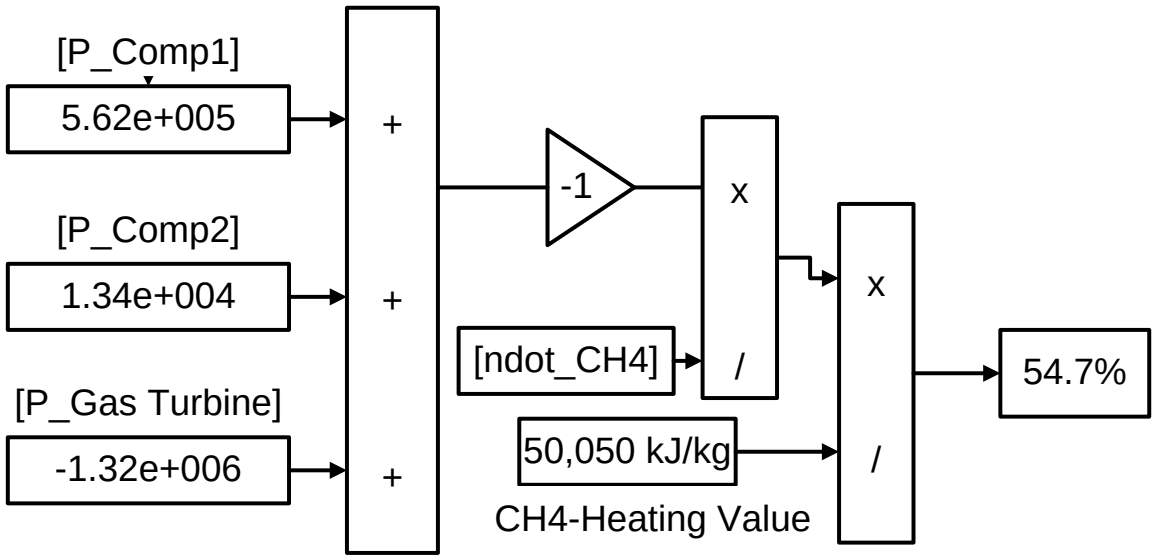

Figure 23: Efficiency of Gas Turbine Cycle

Accordingly, as shown in Figure 23, the thermal efficiency of the cycle is about 55%.

3.3.1.3 Flow, entropy and enthalpy diagram for the complete plant

Figure 24 below shows the flow diagram in the system showing the change in enthalpy, entropy, mass flow rate, and molar flow of each of the gases. Based on the results, we can notice the following:

1. The air and fuel compressors increase the air and fuel temperatures to 784K and 370K, respectively.
2. After mixing the air and fuel, the temperature of the stream reaches up to 770K before the combustion chamber.
3. The combustion chamber then heats the stream to around 2000K before it enters the turbine.
4. The stream leaves the turbine at a temperature of 1150K which is considerably high and it can be used to pre-heat the fuel and air before entering the combustion chamber.

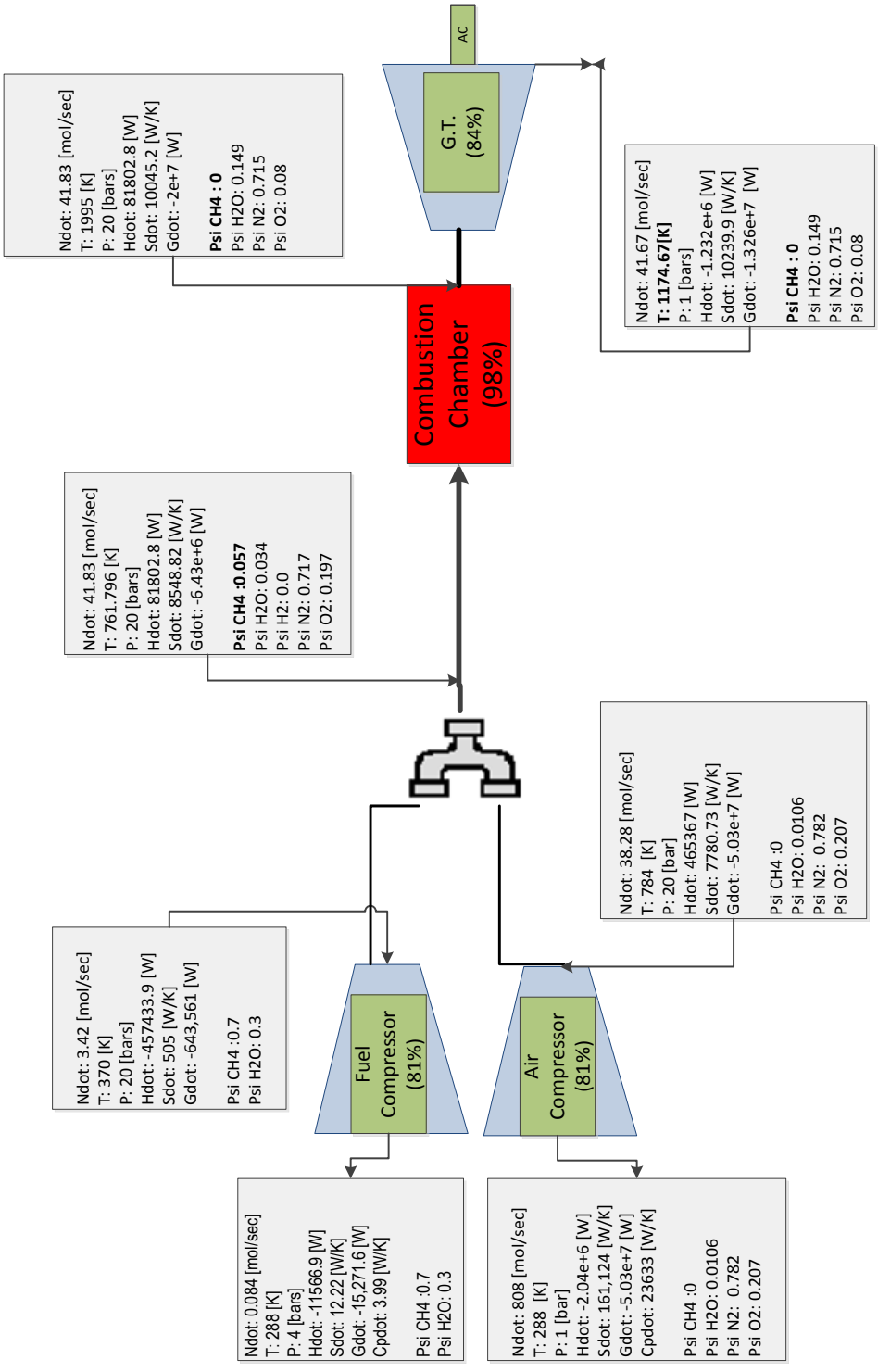

Figure 24: Flow Diagram in Conventional Gas Turbine Cycles

3.3.2 Simulation of the SOFC integrated into Gas turbine Cycle

After the simulation and economic analysis of the SOFC stack, the SOFC was integrated into the gas turbine cycle, and the system was analyzed to maximize the efficiency and the output power.

In order to decide on the ideal layout to integrate the SOFC into the gas turbine cycle, several decisions need to be made to maximize the efficiency and optimize the performance. These decisions include but are not limited to the following:

1. Inlet temperature of fuel at SOFC anode
2. Inlet temperature of air at SOFC cathode
3. Percentage of water content mixed with the CH_4 (fuel)
4. Number of fuel cells in the stack

To start with, the system Simulink layout was done as shown in Figure 25 below:

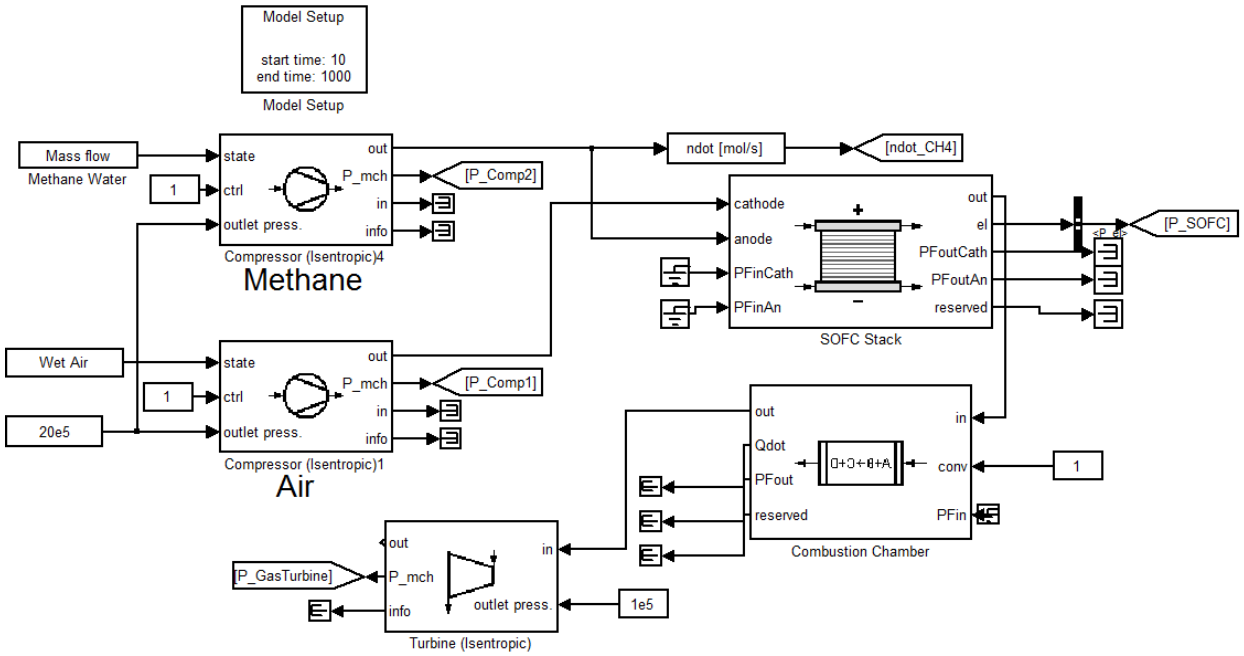

Figure 25: Initial Simulation for the SOFC Stack integrated into Gas Turbine Cycle

As shown in Figure 25, the system consists of two compressors, a fuel compressor which compresses the fuel before it enters at the anode of the SOFC stack and an air compressor which compresses the air before enters at the cathode of the SOFC. The

SOFC preheats the air before it enters the combustion chamber. After that the mixed stream leaving the SOFC stack (which includes a mixture of H_2O, H_2, remaining CH_4, CO_2, and N_2) enters the combustion chamber where it is heated using the unutilized fuel leaving the SOFC.

In order to compare the different systems at the same conditions, the same air and fuel flows and parameters have been applied. The pressure ratio was set to 20 (as concluded from the analyses of the gas turbine cycle) to insure best cycle efficiency.

Furthermore, to maximize the efficiency of the SOFC system and the output power, the system was tested by changing the following decision variables as shown below.

3.3.2.1 Factors affect the performance of the integrated cycle

A. Effect of the water content in the Fuel Flow

As mentioned earlier, in the SOFC cycle the same fuel flow was used in the gas turbine cycle which is 2.5 mol/s. However, an additional parameter needs to be included which is the water content mixed with CH_4. Table 18 below shows the results obtained for the SOFC power at different flow rates of H_2O mixed with CH_4.

Table 18: SOFC Power based on changing the water content

Water Content (mol/sec)	SOFC Power (kW)
0.41	43.7
0.68	52
1	56
1.4	57
2	51
2.9	45

Figure 26 below shows the relationship between the effects of the water content mixed with the fuel and the SOFC power.

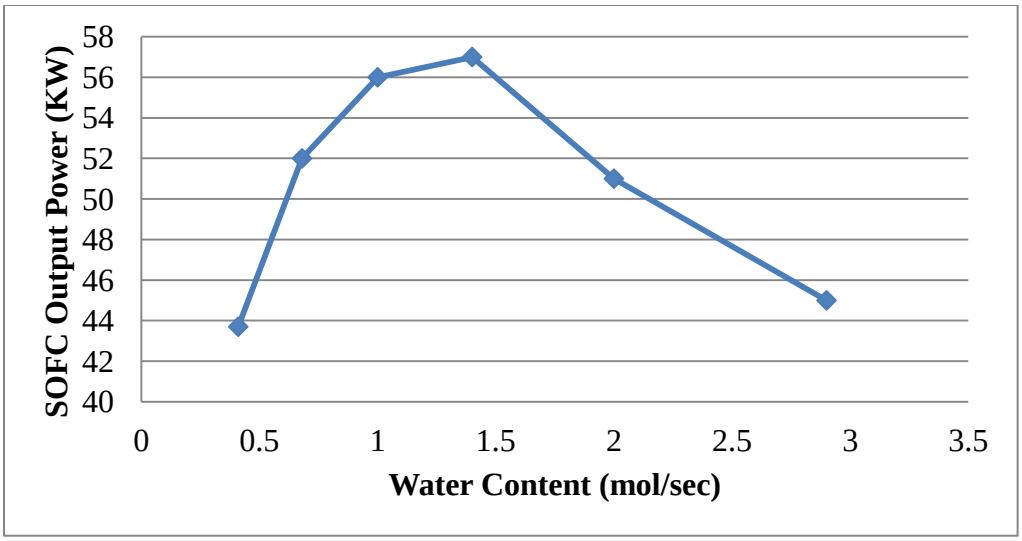

Figure 26: Effect of fuel water content on SOFC power at a fuel flow rate of 2.5 mol/sec

Accordingly, and based on the results shown in Figure 26, the SOFC power is maximized when the water content is 1.4 mol/sec.

B. Effect of the Cathode and Anode Temperature

As discussed earlier in the simulation of the SOFC stack, the SOFC is a high temperature fuel cell stack and it is more efficient at high temperatures. However, a very important issue to consider is that the outlet temperature of the fuel compressor is different than the outlet of the air compressor due to two main reasons:

1. The CH_4 is being supplied for compressed cylinders, so the inlet pressure to the compressor is about 3 bar rather than 1 bar in the air compressor. This means that the CH_4 will be compressed only from 3 to 20 bar (rather than 1 to 20 bar as in the air compressor), which means that the outlet temperature of the fuel compressor is less than the outlet from the air compressor.
2. The molecular flow and the molecular characteristics are different which means that the fuel and air will be leaving the compressors at different temperatures and required different heating energies.

In order to vary the fuel temperature at the inlet of the SOFC anode, and the air temperature at the inlet of the SOFC cathode, heat exchangers have been added to the cycle. Here heat is being utilized from the hot stream leaving the gas turbine to heat the air and fuel leaving both the air and fuel compressors before they enter the SOFC stack.

Accordingly, the system layout has been modified as shown in Figure 27

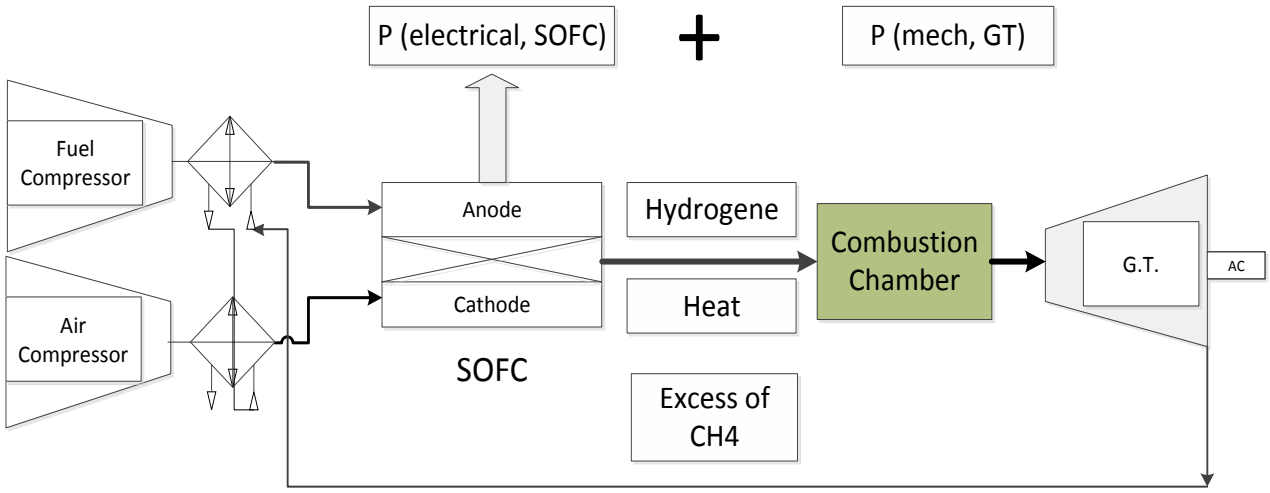

Figure 27: Revised SOFC layout after adding the heat exchangers

As shown in the layout, the hot stream leaving the gas turbine will be fed to the heat exchanger to first pre-heat the fuel before it enters the SOFC anode, and then heat the air before it enters the cathode. The sequence of heating is due to the fact that the fuel requires more heating than the air due to the reasons mentioned in the previous section.

Table 19 shows the results obtained after adding the heat exchangers and simulating the system:

Table 19: SOFC Power based on changing the anode and cathode temperatures

Anode Supply Temperature (K)	**Cathode Supply Temperature (K)**	**SOFC Outlet Temperature (K)**	**SOFC Power (kW)**
350	707	651	57
380	707	660	61
410	707	680	65
535	707	710	87
570	707	715	90
600	707	1125	135
600	800	1150	120
600	840	975	100

Figure 28 below shows a graphical representation of the obtained results.

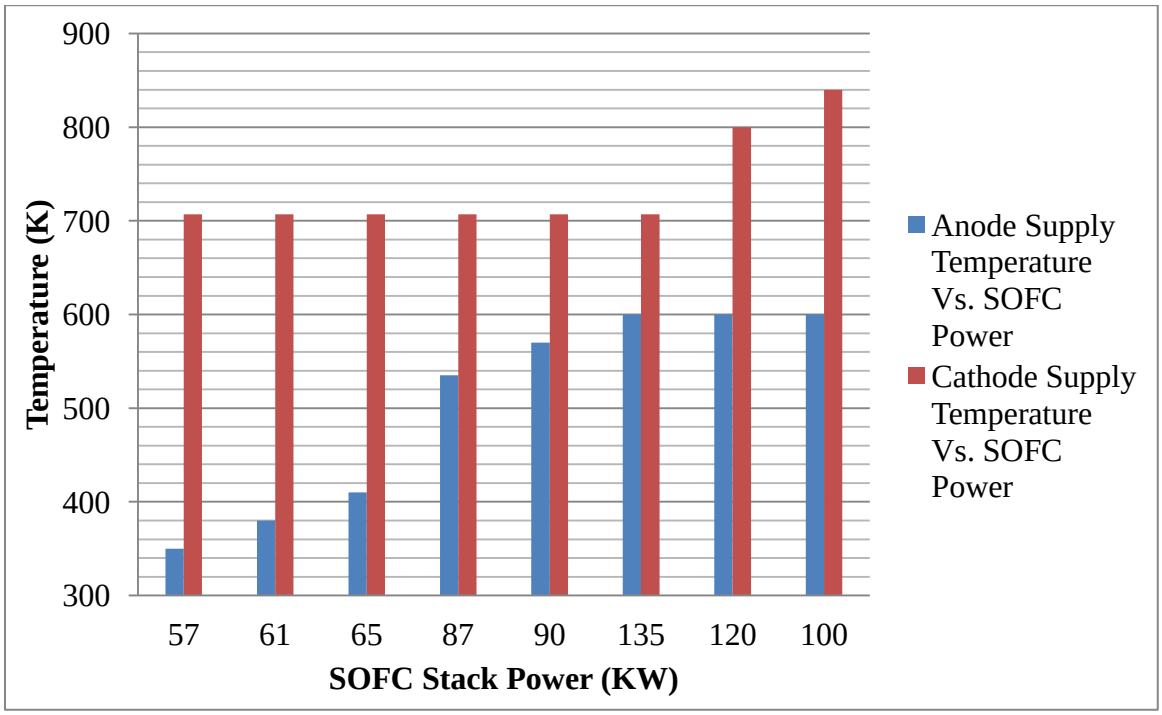

Figure 28: Temperature at the inlet of both the Anode & Cathode of the SOFC Stack versus SOFC Output Electrical Power

From the above results it can be concluded the ideal temperature of fuel entering the anode to obtain maximum efficiency is 600 K. Accordingly, the fuel has to be reheated from a temperature of 350K to 600K before it enters the anode.

However, as the results show, the best SOFC performance is obtained when the air temperature entering the anode is 707K, which is the actual temperature of air leaving the air compressor, which accordingly means that no pre-heat of the air is required before it enters the anode.

Accordingly, the system layout will be revised to include only one heat exchanger to pre-heat the fuel before it enters the anode of the SOFC stack. Figure 29 below shows the revised system layout:

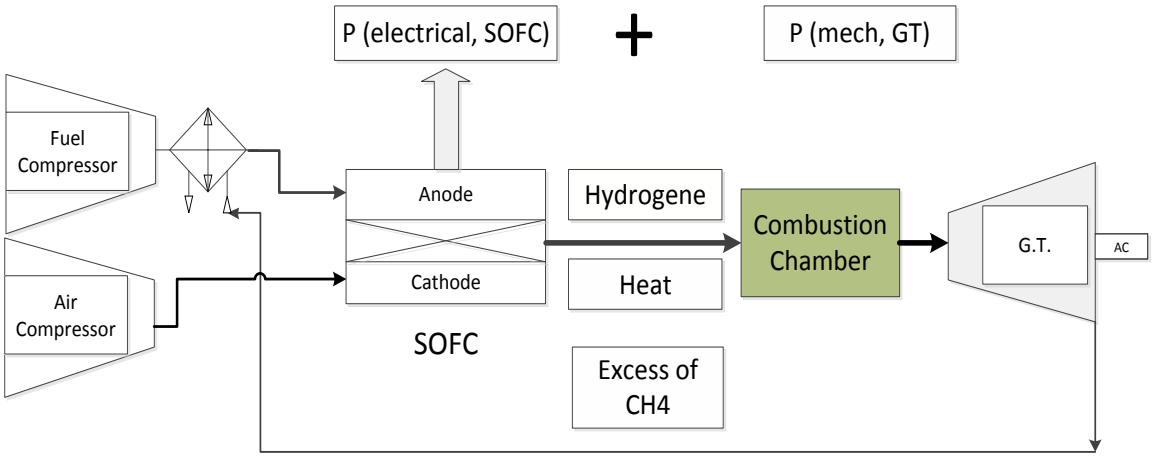

Figure 29: Final SOFC Layout to study System performance

C. Numbers of Cells in the SOFC Stack

The number of cells in the SOFC stack depends on the current rating, voltage rating, and power rating of each of the fuel cells. The fuel cell stack is constructed by connecting the cells in mixed parallel and series connections based on current ratings.

Accordingly, and based on a standard cell area of 0.04 m^2 and a total power rating of 150 kW, a total number of 1000 fuel cells will be used to build the stack, and this setting shall be added to the configuration of the fuel cell stack in the Simulink Model as shown in Figure 30 below.

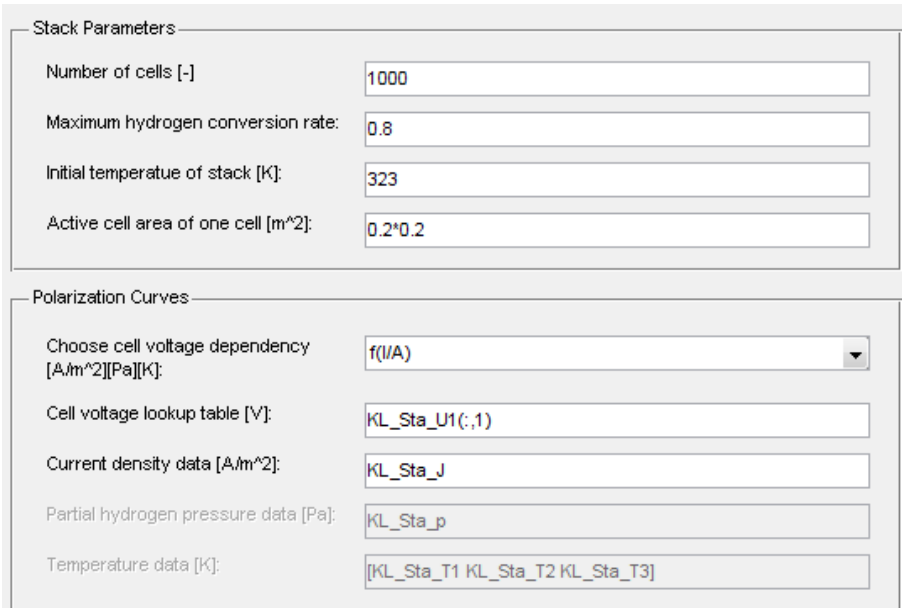

Figure 30: SOFC Stack Configuration

3.3.2.2 Thermal Efficiency of the plant

Figure 31 shows the final Simulink model of the SOFC system integrated into the gas turbine cycle.

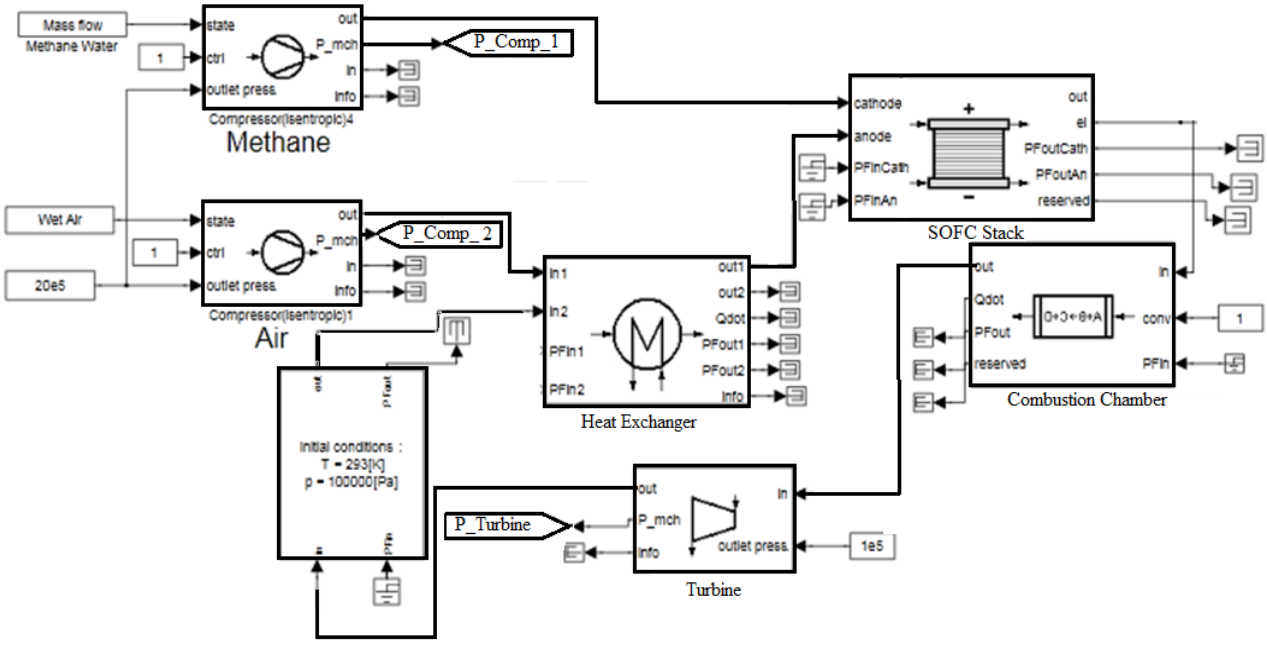

Figure 31: Final Simulink Model of SOFC integrated into Gas turbine Cycle

Figure 32 below shows the final optimized results obtained after simulating the SOFC system integrated into the gas turbine cycle.

$$\eta = \frac{P_{mech.GT} + P_{SOFC,elec} - P_{Fuel\ Comp} - P_{Air\ Comp}}{\dot{m}_{fuel} \times LHV_{CH4}} \quad (34)$$

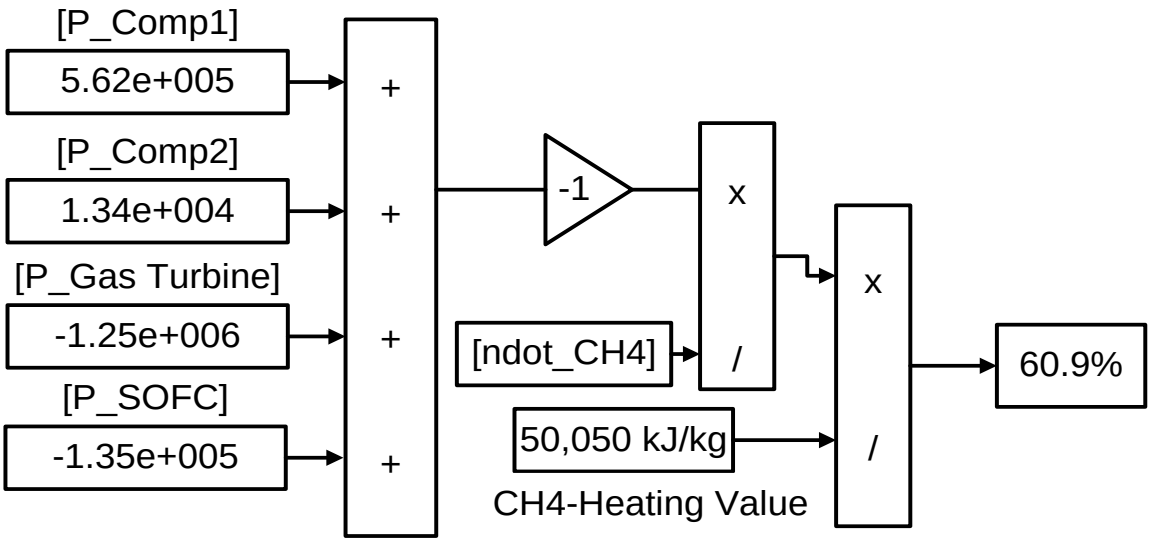

Figure 32: Efficiency calculations of the Gas Turbine and SOFC System

As shown in Figure 32, the overall thermal efficiency has increased to 61%.

3.3.2.3 Flow, entropy and enthalpy diagram for the complete plant

Figure 33 below shows the flow diagram in the system showing the change in enthalpy, entropy, mass flow rate, and molar flow of each of the gases. Based on the results shown we can notice the following:

A. Fuel leaves the fuel compressor at a temperature of 370K then gets pre-heated using the heat exchanger to a temperature of 616K.
B. Air leaves the air compressor at a temperature of 780K.
C. The mixture of air and fuel leaves the SOFC stack at 820K.
D. Hydrogen is produced from the reactions inside the SOFC.
E. There is an excess of CH_4 leaving the SOFC stack which is used in the combustion chamber to heat the stream before it enters the gas turbine.
F. The air enters the turbine at 1850K and leaves at 1050K and is used to pre-heat the fuel before it enters the SOFC stack.

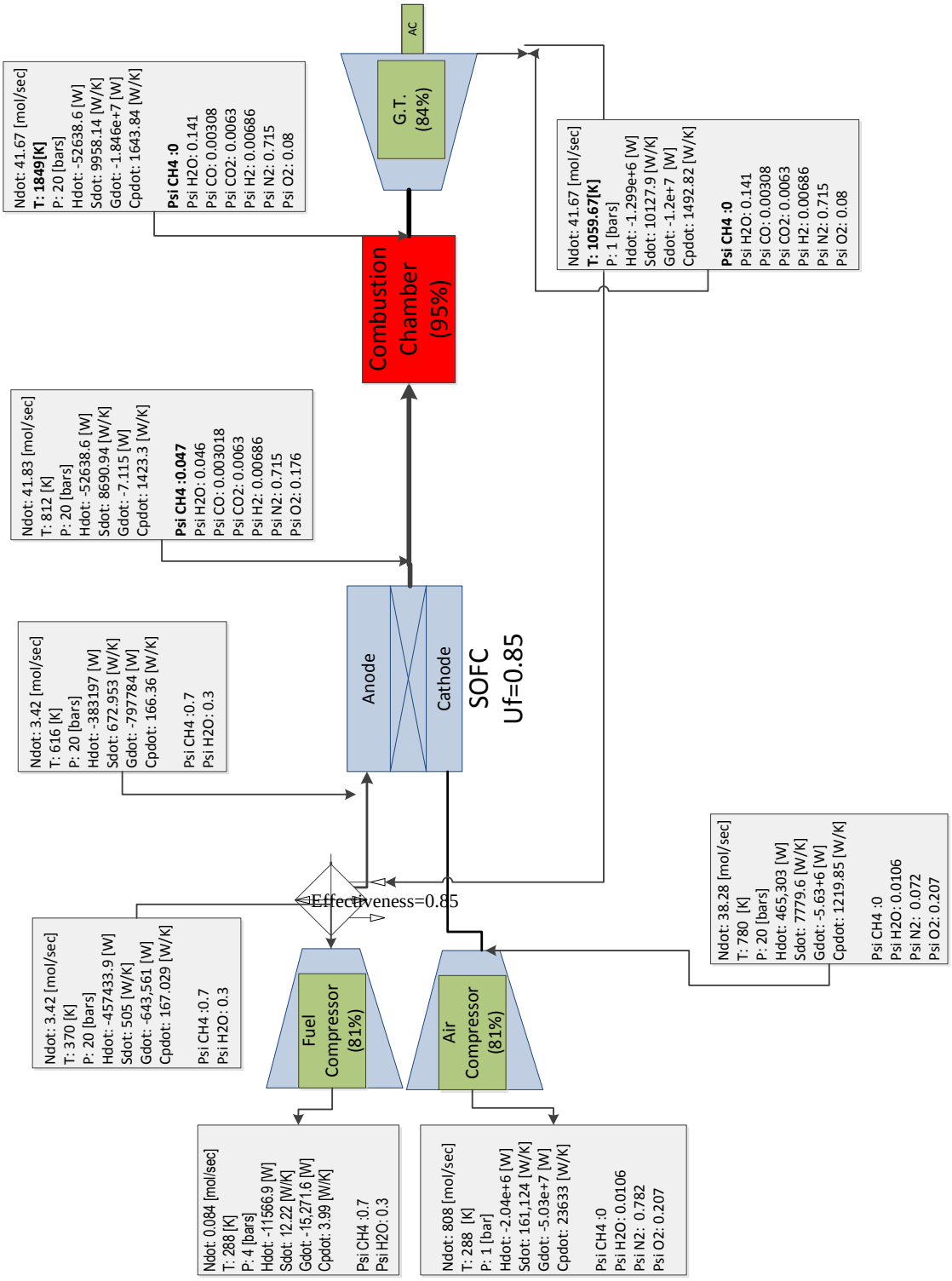

Figure 33: Flow Diagram in SOFC-Gas Turbine Cycle

3.3.3 Simulation of the PEMFC integrated into Gas turbine Cycle

The last system to study is the proposed system which is to integrate the PEMFC into the SOFC-gas turbine cycle.

As mentioned earlier, in order to integrate PEMFC into the SOFC-gas turbine cycle, the PEMFC shall utilize the excess hydrogen produced from the SOFC stack. Furthermore, since the PEMFC is a medium-temperature fuel cell, and with reference to the results obtained in section 2.1.3, the ideal operating temperature of the PEMFC stack is between 400-440 K. Accordingly, since the gas mixture leaves the SOFC at a temperature of 850 K and directly enters the PEMFC, a pre-cooling is required for the mixture before it enters the PEMFC.

3.3.3.1 PEMFC Stack configuration

The PEMFC stack is characterized using its will-know polarization curve which is determined using fixed relationships which are specified to demonstrate a low temperature PEMFC.

The PEMFC stack is assumed to have a thermal mass operating at uniform temperature and exchanging heat with the flow streams going through the anode and cathode of the stack. The value of this thermal mass is defined in the configuration of the stack. The flows leaving both the cathode and the anode of the stack have the same temperature, which is the "stack temperature."

It is also assumed that there is no heat loss to the environment during the operation and that the stack temperature is calculated using energy balance.

In addition to this, the humidity of the stack is calculated using the average value of the relative humidity of the anode and the cathode inlets/outlets. The relation between this average relative humidity and the water content of the stack is given in the lookup table where the first row is the relative humidity, and the second row is the membrane water content (0 dry, 14 wet).

Since the flow stream entering the anode of the PEMFC stack is leaving the SOFC at a high temperature, cooling is required. Cooling is done by an input flow that acts as a cooling medium for the stack.

Figure 34 below shows the PEMFC stack block which is integrated into the complete cycle.

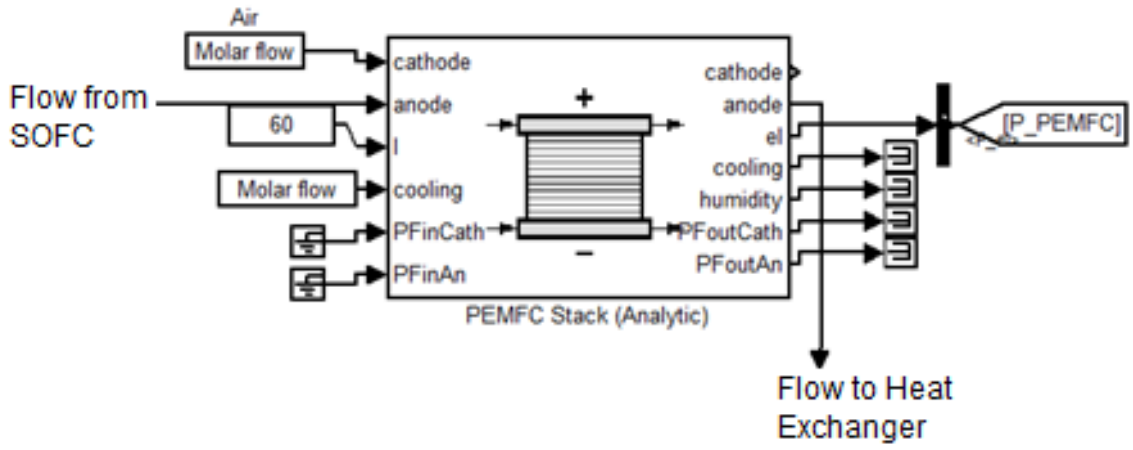

Figure 34: PEMFC stack Simulink block

As shown in Figure 34, the operation of the PEMFC stack is governed by varying several parameters which are the molar flow at the cathode, the molar flow for cooling, and the control current.

Figure 35 below shows the configuration parameters for the molar air flow entering the PEMFC cathode.

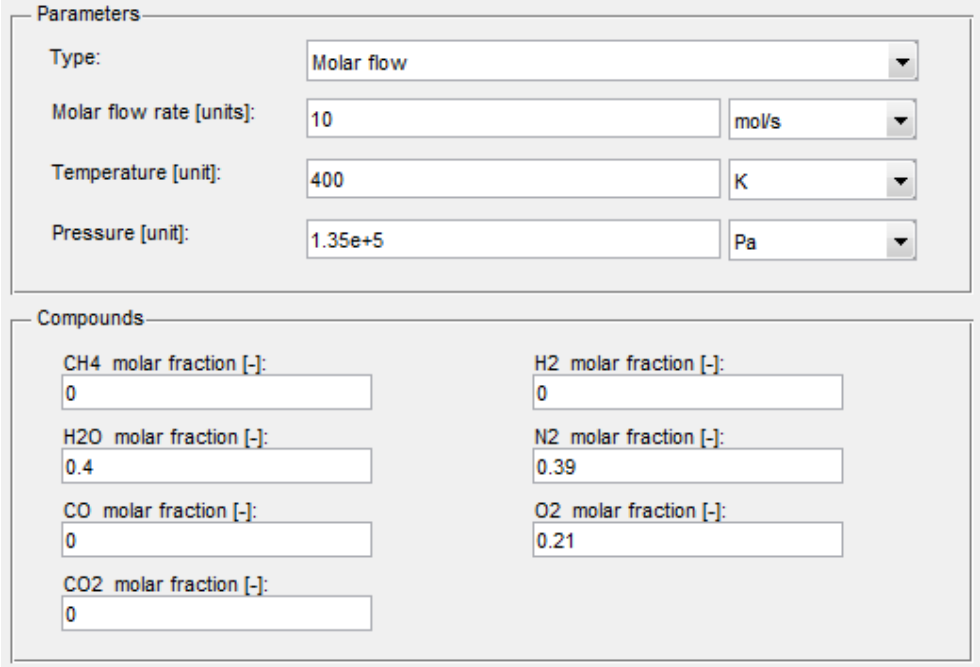

Figure 35: Configuration Parameters for Molar flow for PEMFC Cathode

Moreover, Figure 36 below shows the configuration parameters for the molar flow for PEMFC cooling.

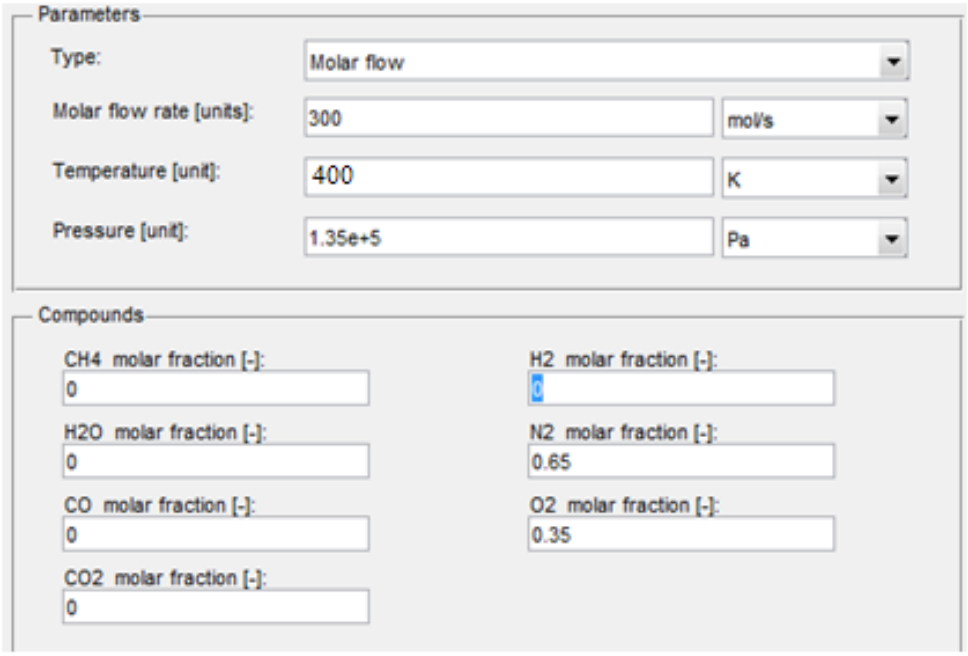

Figure 36: Configuration Parameters for Molar flow for PEMFC Cooling

Finally, and based on the results obtained in Chapter 2 for PEMFC simulation, Figure 37 below shows the configuration parameters for the PEMFC stack including the number of cells, initial temperature, and the cell area.

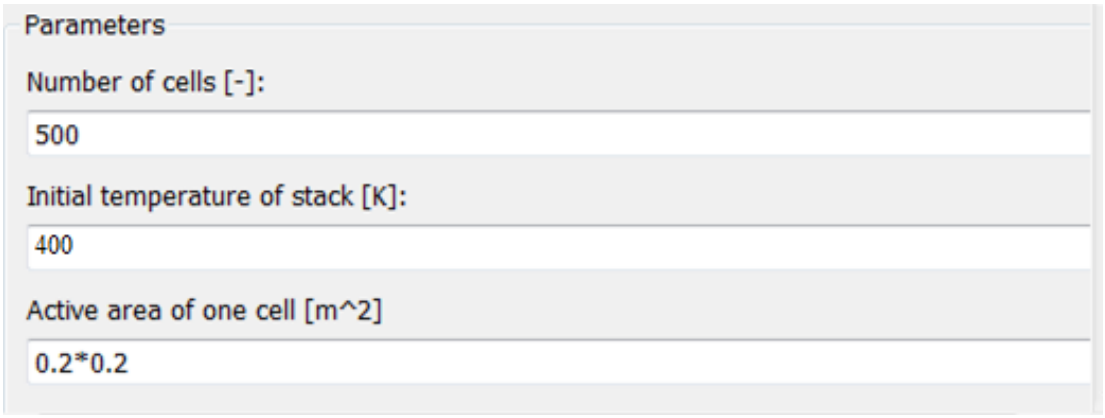

Figure 37: Configuration Parameters for PEMFC Stack

3.3.3.2 Integrated cycle after adding the PEMFC Stack

The Simulink model of the integrated cycle is shown in Figure 38 below:

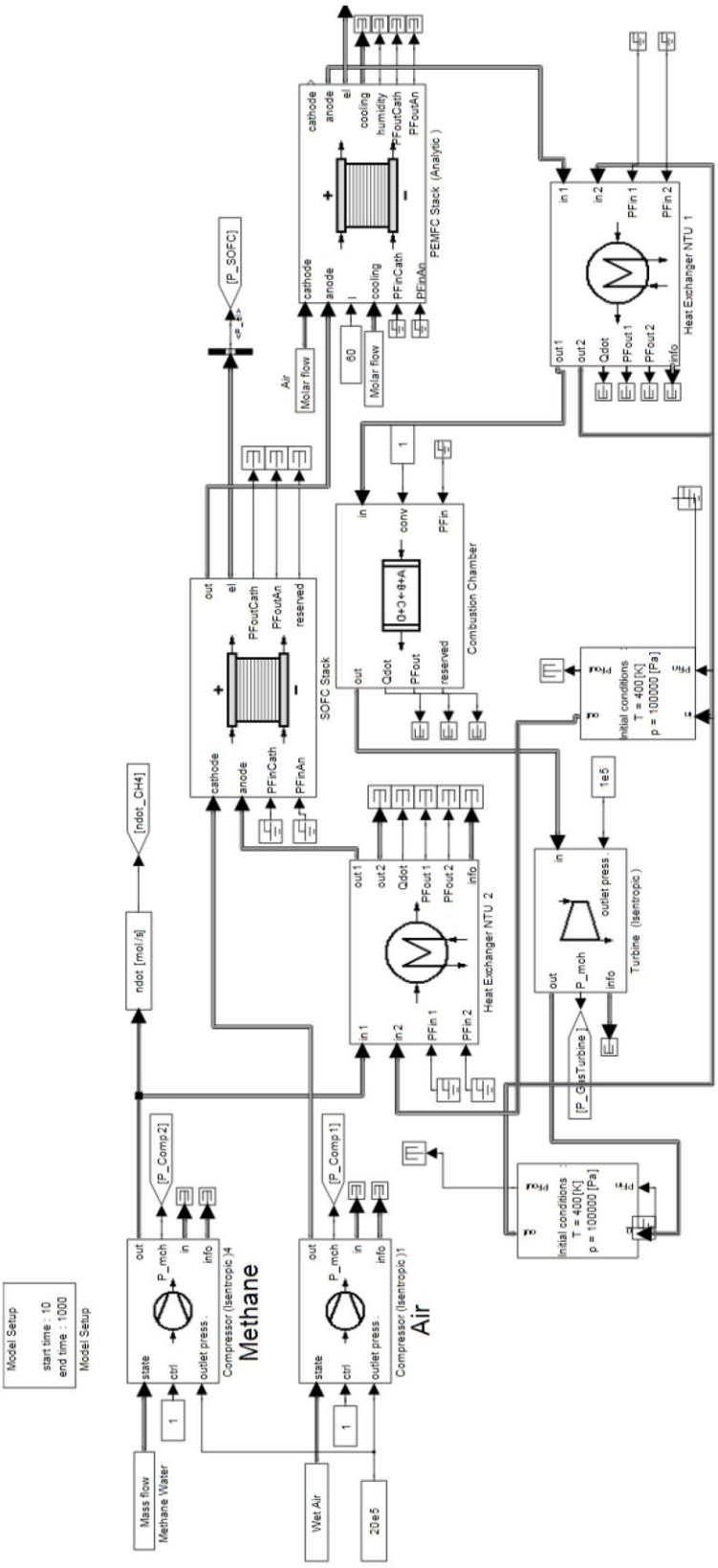

Figure 38: Simulink Model of PEMFC & SOFC in Gas Turbine Cycle

In order to operate the system after integrating the PEMFC Stack, an additional heat exchanger was added to the system to utilize the thermal energy of the flow exiting the turbine to preheat the relatively cold air leaving the PEMFC before entering the combustion chamber. The final layout of the system is shown in Figure 39.

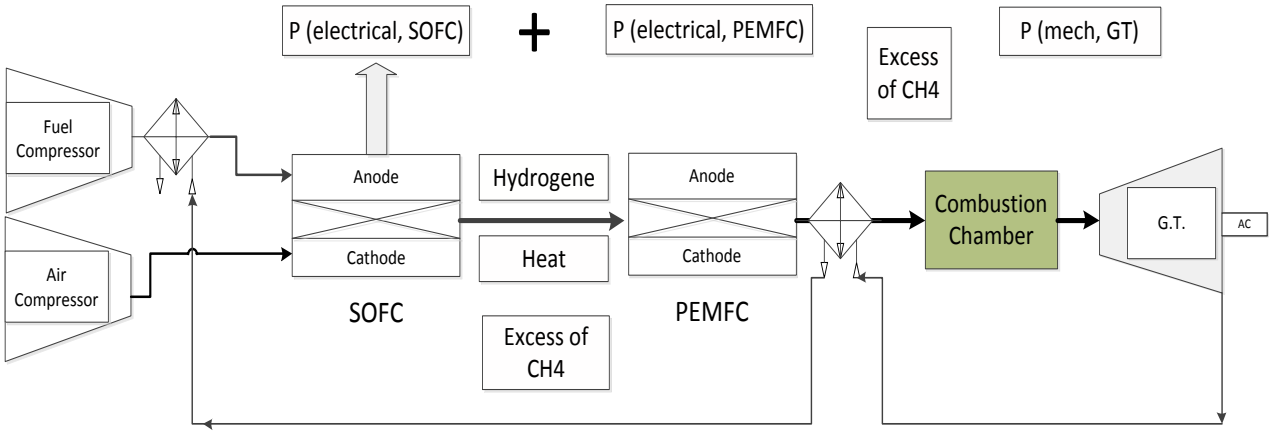

Figure 39: PEMFC Layout after Adding Heating Exchanger before the Combustion Chamber

3.3.3.3 Thermal efficiency of the integrated cycle

Figure 40 below shows the net power output and the final result of the efficiency.

$$\eta = \frac{P_{mech.GT} + P_{SOFC,elec} + P_{PEMFC,elec} - P_{Fuel\ Comp} - P_{Air\ Comp}}{\dot{m}_{fuel} \times LHV_{CH4}} \quad (35)$$

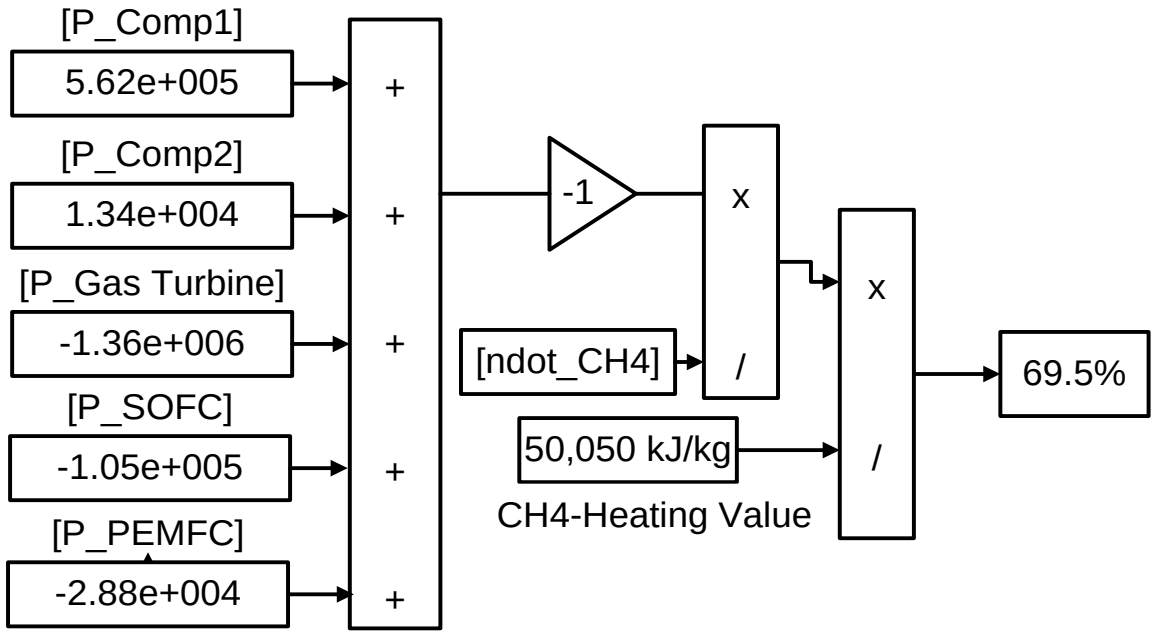

Figure 40: PEMFC & SOFC- Gas Turbine Cycle efficiency

As shown in Figure 40, by integrating the PEMFC we have reached an efficiency of about 70% and a net power of 1 MW.

3.3.3.4 Flow, entropy and enthalpy diagram for the complete plant

Figure 41 below shows the enthalpy, entropy and mass flow rates across the complete cycle. Based on the results shown the following can be concluded:

A. The flow stream leaves the SOFC at a temperature of 770K after which the stream is directed to the PEMFC.
B. The flow is being cooled internally in the PEMFC stack and then the H_2 which is produced in the SOFC stack is being used as a fuel to produce electricity.
C. The stream leaves the PEMFC at 403K and then gets pre-heated in the heat exchanger using the hot flow stream leaving the gas turbine to a temperature of 936K.
D. Since the excess CH_4 which has left the SOFC stack is still not utilized, this excess fuel is now used in the combustion chamber to heat the stream to a temperature of 2000K.
E. The flow stream leaves the turbine at a temperature of 1170K which is considerably high and enough to pre-heat the air leaving the SOFC then also heat the fuel leaving the fuel compressor.

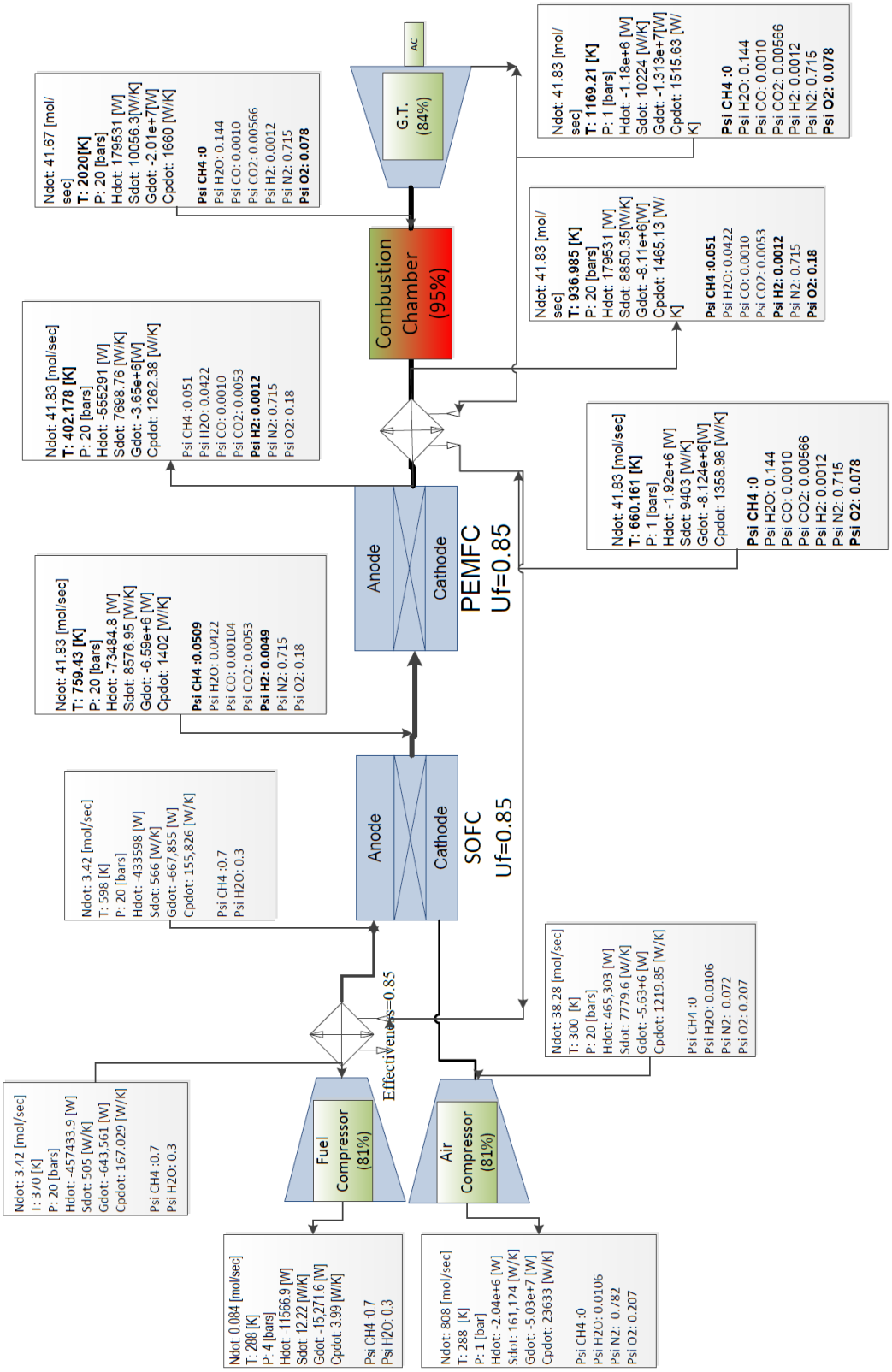

Figure 41: Flow Diagram in PEMFC+ SOFC-Gas Turbine Cycle

3.4 2nd Law Analysis of the Integrated Gas Turbine Systems

3.4.1 Exergy Equations for compressor, gas turbine and heat exchangers

In order to perform 2nd law analyses on the proposed systems, the exergy destruction and the exergitic efficiency was calculated for each of the system's components. To start with, the equations of the exergy destruction have been derived for the compressor, gas turbine, and heat exchanger and were tabulated as shown in Table 20 below [20].

Table 20: Exergy equations for the compressor, turbine, and heat exchanger

Compressor	Exergy destruction	$\dot{E}_{x,dest,C} = \dot{W}_C - \dot{m}_{in}(e_{x,out} - e_{x,in})$	(36)
	Exergy efficiency	$\eta_{exe,C} = \frac{\dot{m}_{in}(e_{x,out} - e_{x,in})}{\dot{W}_C}$	(37)
Gas Turbine	Exergy destruction	$\dot{E}_{x,dest,GT} = \dot{m}_{in}(e_{x,in} - e_{x,out}) - \dot{W}_{GT}$	(38)
	Exergy efficiency	$\eta_{exe,GT} = \frac{\dot{W}_{GT}}{\dot{m}_{in}(e_{x,in} - e_{x,out})}$	(39)
Heat Exchanger	Exergy destruction	$\dot{E}_{x,dest,HX} = \dot{m}_{in,2}(e_{x,in,2} - e_{x,out,2}) - \dot{m}_{out,1}(e_{x,out,1} - e_{x,out,1})$	(40)
	Exergy efficiency	$\eta_{exe,HX} = \frac{\dot{m}_{out,1}(e_{x,out,1} - e_{x,out,1})}{\dot{m}_{in,2}(e_{x,in,2} - e_{x,out,2})}$	(41)

3.4.2 Exergy Equations for Fuel Cell Stacks

Furthermore, in order to derive the exergy equations for the fuel cell stack, the following procedure was followed:

The mass balance for the SOFC gives:

$$\sum_{in} mass\ flows = \sum_{out} mass\ flows$$

Thus,

$$\begin{aligned} \dot{m}_{cthode} + \dot{m}_{fuel,FC} &= \dot{m}_{SOFC,out} \\ &= \dot{m}_{cthode} + \dot{m}_{fuel,FC} \times U_f + \dot{m}_{fuel,FC}(1 - U_f) \end{aligned} \tag{42}$$

The last part of the equation represents the non-reacted mass flow which leaves the SOFC downstream of the products.

Accordingly, based on the first law of thermodynamics:

$$\begin{aligned} \dot{m}_{cthode} h_{cathode} + \dot{m}_{fuel,FC} \times U_f \times LHV + \dot{m}_{fuel,FC}(1 - U_f) h_{fuel,in} \\ - \dot{W}_{FC} - \dot{m}_{out} h_{out} = 0 \end{aligned} \tag{43}$$

Accordingly, the exergy balance can be written as shown below:

$$\begin{aligned} \dot{m}_{cthode} e_{cathode} + \dot{m}_{fuel,FC} e_f^{PH} + \dot{m}_{fuel,FC} U_F e_f^{CH} - \dot{W}_{FC} - \dot{m}_{out} e_{out} \\ - \dot{E}_{x,dest,FC} = 0 \end{aligned} \tag{44}$$

where e_f^{PH}, e_f^{CH} are the physical and chemical exergies of the fuel utilized.

Hence, the exergy efficiency can be written as:

$$\eta_{exe,FC} = \frac{\dot{W}_{FC}}{\dot{m}_{cthode} e_{cathode} + \dot{m}_{fuel,FC} e_f^{PH} + \dot{m}_{fuel,FC} U_F e_f^{CH} - \dot{m}_{out} e_{out}} \tag{45}$$

Furthermore, the PEMFC exergy equations can be derived by considering both the physical and chemical exergies.

The physical exergy is related to the temperature and pressure of the fluids and the reactants in the fuel cell stack. The physical exergy can be written in terms of the enthalpy and entropy, assuming that T_0 = 288 K and P_0= 1 atm. Accordingly, the physical exergy can be calculated using the following equation: [21]

$$e^{PH} = (h - h_0) - T_0(s - s_0) \quad (46)$$

where h_0 and s_0 are the specific enthalpy and entropy at standard conditions. Eventually, to calculate the physical exergy of an ideal gas with a constant specific heat C_p and specific ration k, the following equation can be used:

$$e^{PH} = C_P T_0 [\frac{T}{T_0} - 1 - \ln\left(\frac{T}{T_0}\right) + \ln (\frac{P}{P_0})^{\frac{k-1}{k}} \quad (47)$$

On the other hand, the chemical exergy is related to the chamical reactions in the system. In general, the chemical exergy is calculated based on standard values T_0 = 288 K, and P_0 = 1 atm.

3.4.3 Exergy Equations for Combustion Chamber

The equations below show the procedure followed to perform exergy analysis for the combustion chamber in each of the three cycles [22]:

$$\dot{m}_{inlet} e_{inlet} + \dot{m}_{fuel,Comb}\left(e_f^{PH} + e_f^{CH}\right) + \dot{m}_{fuel,FC}(1 - U_F) e_f^{CH} - \dot{m}_{out} e_{out} - (1 - \frac{T_0}{T_{sink}})\dot{Q}_{loss} - \dot{E}_{x,dest,Comb} = 0 \quad (48)$$

$$\eta_{exe,Comb} = \frac{\dot{m}_{out} e_{out} - \dot{m}_{inlet} e_{inlet}}{\dot{m}_{fuel,Comb}\left(e_f^{PH} + e_f^{CH}\right) + \dot{m}_{fuel,FC}(1 - U_F) e_f^{CH}} \quad (49)$$

3.4.4 Exergy Equations for Integrated Systems

Equations 3.18 and 3.19 show the equations used to calculate exergy destruction and 2nd l law efficiency for each of the integrated systems [21]:

$$\dot{m}_{inlet} e_{inlet} + \dot{m}_{fuel}\left(e_f^{PH} + e_f^{CH}\right) - \dot{m}_{out} e_{out} - \dot{W}_{net} - \dot{E}_{x,dest} = 0 \quad (50)$$

$$\eta_{ex}^{Cyc} = \frac{\dot{W}_{net}}{\dot{m}_{fuel}\left(e_f^{PH} + e_f^{CH}\right)} \quad (51)$$

Finally, Table 21 below shows the properties used in to perform the analysis.

Table 21: operating conditions used to perform exergy analysis [30]

Property	**Value**
Standard Temprature, T_0	288 K
Standard pressure, P_0	1 atm
Average specific heat of air, C_p	1.005 kJ/kg.K
Average specific heat of hydrogene, C_p	14.3 kJ/kg.K
Specific hear ratio for air and hydrogen, k	1.4
Enthalpy of water at standard condition	104.88 kJ/kg
Entropy of water and standard condition	0.366 kJ/kg.K
Enthalpy of air at standard condition	-21,120 kJ/kmol
Entropy of air at standard condition	129.17 kJ/kmol.K
Compressor Efficiency	81%
Turbine Efficiency	84%
Heat exchanger effectiveness	85%
Combustor efficiency	98%
Fuel utilization factor	0.85
SOFC Stack temperature	750 K
PEMFC stack temperature	420 K

3.4.5 Exergy Calculations' results

Tables 22, 23, and 24 below show the results obtained from the exergy calculations using the equations derived in the previous sections. They also display the results obtained from the simulation and which are shown in the flow diagrams of each of the systems under study.

Table 22: Exergy Calculations for Conventional Gas Turbine System

Component	**Exergy Destruction (W)**	**2nd Law Efficiency (%)**
Fuel Compressor	2,226.5	80%
Air Compressor	43,000	81%
Combustion Chamber	456,231	76%
Gas Turbine	67,562	82%

Table 23: Exergy Calculations for SOFC Integrated into Gas Trubine Cycle

Component	**Exergy Destruction (W)**	**2nd Law Efficiency (%)**
Fuel Compressor	2,080	80%
Air Compressor	43,000	81%
Combustion Chamber	388,640	78%
Gas Turbine	50,235	83%
SOFC Stack	67,690	81%
Heat Exchanger	7,496	82%

Table 24: Exergy Calculations for PEMFC + SOFC integrated into Gas Turbine Cycle

Component	**Exergy Destruction (W)**	**2nd Law Efficiency (%)**
Fuel Compressor	2,080	80%
Air Compressor	43,000	81%
Combustion Chamber	371,575	80%
Gas Turbine	38,614.84	87%
SOFC Stack	67,690	81%
PEMFC Stack	7,000	79%
Heat Exchanger 2	21,500	78%
Heat Exchanger 1	7,496	82%

Table 25 below shows the summary of the exergy analysis of each of the systems under study.

Table 25: Summary of Exergy destructions and 2nd Law efficiencies

System	Total Exergy Destruction (kW)	Net Power Output (kW)	2nd Law Efficiency
Conventional Gas Turbine Cycle	566	720	56.2%
SOFC Integrated in Gas Turbine Cycle	559	800	59%
PEMFC & SOFC Integrated into Gas Turbine Cycle	554	920	62.4%

Chapter 4: Technology Management of the Proposed Systems

Figure 42 below shows the procedure and the main points to be considered in order to study the economics of the proposed systems.

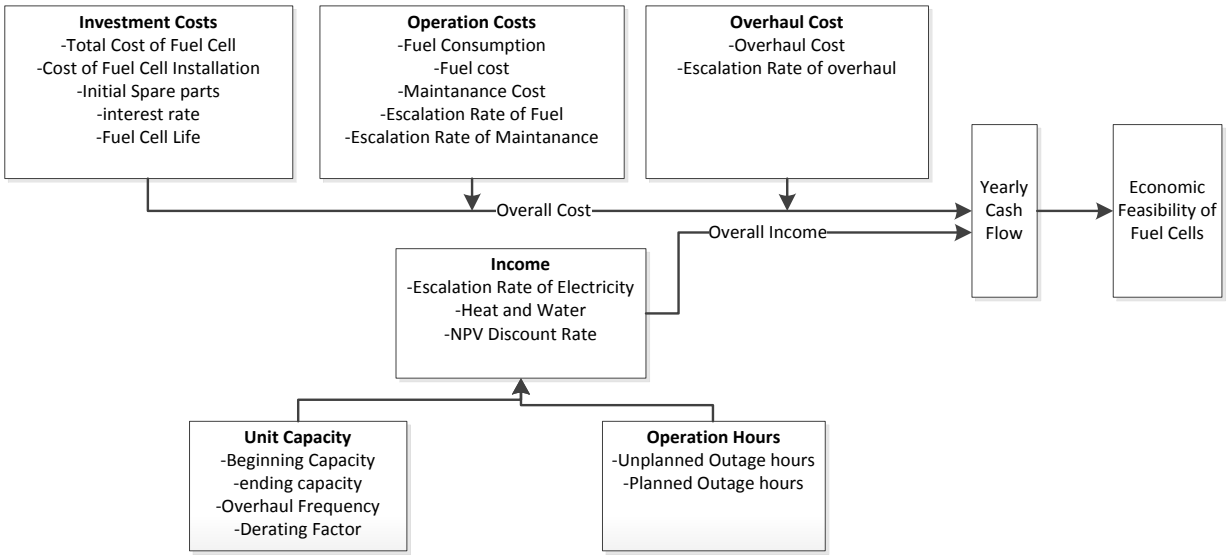

Figure 42: Steps to Study the Economic Feasibility of Fuel Cells

4.1 Capital cost calculations

In order to compare the three proposed systems, the first step would be to estimate the capital cost for all the equipment used and all other costs associated with operation and maintenance. [13]

The equations used to calculate the capital costs for the heat exchangers, gas turbine, and compressors are as shown below:

$$C_{HX} = 130\left(\frac{A_{HX}}{0.093}\right)^{0.78} \quad (52)$$

$$C_{GT} = W_{GT}[131.85 - 98.32\ln(W_{GT})] \quad (53)$$

$$C_{COMP} = 91{,}562\left(\frac{W_{comp}}{445}\right)^{0.67} \quad (54)$$

Using the equations above and the calculations done in the previous sections, Table 26 below shows the obtained results: [14] and [15]

Table 26: Initial cost for each of the mechanical components in the integrated cycle

Item	Cost
Air Compressor	$97, 534
Fuel Compressor	$12,000
Gas Turbine	$547,320
SOFC Stack (2000 $/kW)	$200,000
PEMFC Stack (2000 $/kW)	$60,000
Heat Exchangers 1	$2000
Heat Exchanger 2	$6000
Combustion Chamber	$50,000
Annual Fuel Cost	$125,000

Table 27 below shows the estimated capital costs for each of the three systems under study after integrating all the system components.

Table 27: Capital costs for each of the three systems under study

System	Capital Cost (USD)
Gas Turbine Cycle	$1,009,000
Gas Turbine+ SOFC	$1,209,000
Gas Turbine +SOFC+PEMFC	$1,306,000

4.2 Economic Evaluation of Conventional Gas Turbine Cycle

To evaluate the system economically, the NPV of the cycle should be calculated taking into consideration the capital cost, Operation and Maintenance cost and selling price of electricity.

The lifetime of a conventional gas turbine cycle is assumed to be 25 years; accordingly, Table 28 below shows the detailed cash flow for the system for its complete lifetime. The analysis has been done based on an interest rate of 5% and an inflation rate of 4%.

Table 28: Cash flow analysis for the Conventional Gas Turbine Cycle

Year	INFLOW (USD)	O&M Cost (USD)	Net Cash Flow (USD)
0	($1,000,000.00)		($1,000,000.00)
1	$1,082,648.40	$220,000.00	$862,648.40
2	$1,125,954.34	$228,800.00	$897,154.34
3	$1,170,992.51	$237,952.00	$933,040.51
4	$1,217,832.21	$247,470.08	$970,362.13
5	$1,266,545.50	$257,368.88	$1,009,176.62
6	$1,317,207.32	$267,663.64	$1,049,543.68
7	$1,369,895.61	$278,370.18	$1,091,525.43
8	$1,424,691.44	$289,504.99	$1,135,186.45
9	$1,481,679.09	$301,085.19	$1,180,593.90
10	$1,540,946.26	$313,128.60	$1,227,817.66
11	$1,602,584.11	$325,653.74	$1,276,930.37
12	$1,666,687.47	$338,679.89	$1,328,007.58
13	$1,733,354.97	$352,227.09	$1,381,127.88
14	$1,802,689.17	$366,316.17	$1,436,373.00
15	$1,874,796.74	$380,968.82	$1,493,827.92
16	$1,949,788.60	$396,207.57	$1,553,581.03
17	$2,027,780.15	$412,055.87	$1,615,724.28
18	$2,108,891.35	$428,538.11	$1,680,353.24
19	$2,193,247.01	$445,679.63	$1,747,567.38
20	$2,280,976.89	$463,506.82	$1,817,470.07
21	$2,372,215.97	$482,047.09	$1,890,168.88
22	$2,467,104.60	$501,328.98	$1,965,775.62
23	$2,565,788.79	$521,382.13	$2,044,406.66
24	$2,668,420.34	$542,237.42	$2,126,182.92
25	$2,775,157.15	$563,926.92	$2,211,230.23
		NPV	**$16,528,255.78**

4.3 Economic Evaluation of SOFC-Gas Turbine Cycle

As discussed earlier, the lifetime of the SOFC stack is assumed to be 5 years; accordingly, the SOFC stack will be replaced every 5 years which will affect the O&M cost. The complete calculation for the NPV is shown in Table 29 below. As the table shows, the O&M cost changes every 5 months to accommodate for the cost of replacing the SOFC stack which is $100,000. The analysis has been done based on an interest rate of 5% and an inflation rate of 4%.

Table 29: Cash flow analysis for the SOFC-Gas Turbine Cycle

Year	INFLOW (USD)	O&M Cost (USD)	Net Cash Flow (USD)
0	($1,00,000.00)		($1,200,000.00)
1	$1,201,784.40	$220,000.00	$981,784.40
2	$1,249,855.78	$228,800.00	$1,021,055.78
3	$1,299,850.01	$237,952.00	$1,061,898.01
4	$1,351,844.01	$247,470.08	$1,104,373.93
5	$1,405,917.77	**$457,368.88**	$948,548.89
6	$1,462,154.48	$267,663.64	$1,194,490.84
7	$1,520,640.66	$278,370.18	$1,242,270.48
8	$1,581,466.28	$289,504.99	$1,291,961.29
9	$1,644,724.94	$301,085.19	$1,343,639.75
10	$1,710,513.93	**$513,128.60**	$1,197,385.33
11	$1,778,934.49	$325,653.74	$1,453,280.75
12	$1,850,091.87	$338,679.89	$1,511,411.98
13	$1,924,095.54	$352,227.09	$1,571,868.45
14	$2,001,059.37	$366,316.17	$1,634,743.20
15	$2,081,101.74	**$580,968.82**	$1,500,132.92
16	$2,164,345.81	$396,207.57	$1,768,138.24
17	$2,250,919.64	$412,055.87	$1,838,863.77
18	$2,340,956.43	$428,538.11	$1,912,418.32
19	$2,434,594.69	$445,679.63	$1,988,915.06
20	$2,531,978.47	**$663,506.82**	$1,868,471.65
21	$2,633,257.61	$482,047.09	$2,151,210.52
22	$2,738,587.92	$501,328.98	$2,237,258.94
23	$2,848,131.43	$521,382.13	$2,326,749.30
24	$2,962,056.69	$542,237.42	$2,419,819.27
25	$3,080,538.96	$563,926.92	$2,516,612.04
		NPV	**$18,317,590.15**

4.4 Economic Evaluation of PEMFC & SOFC Integrated into Gas Turbine Cycle

Table 30 below shows the calculations of the NPV of the proposed system with the PEMFC and SOFC integrated into the gas turbine cycle. The assumed lifetime of the PEMFC is 4 years, which means that in addition to the annual O&M, the cost of replacing the SOFC stack every 5 years, the cost of the PEMFC shall also be added every 4 years which is $50,000. The analysis has been done based on an interest rate of 5% and an inflation rate of 4%.

Table 30: Cash flow analysis for the PEMFC & SOFC-Gas Turbine Cycle

Year	INFLOW (USD)	O&M Cost (USD)	Net Cash Flow (USD)
0	($1,300,000.00)		($1,300,000.00)
1	$1,368,574.80	$220,000.00	$1,148,574.80
2	$1,423,317.79	$228,800.00	$1,194,517.79
3	$1,480,250.50	$237,952.00	$1,242,298.50
4	$1,539,460.52	**$297,470.08**	$1,241,990.44
5	$1,601,038.94	**$457,368.88**	$1,143,670.06
6	$1,665,080.50	$267,663.64	$1,397,416.86
7	$1,731,683.72	$278,370.18	$1,453,313.54
8	$1,800,951.07	**$339,504.99**	$1,461,446.08
9	$1,872,989.11	$301,085.19	$1,571,903.92
10	$1,947,908.68	**$513,128.60**	$1,434,780.08
11	$2,025,825.03	$325,653.74	$1,700,171.28
12	$2,106,858.03	**$388,679.89**	$1,718,178.13
13	$2,191,132.35	$352,227.09	$1,838,905.26
14	$2,278,777.64	$366,316.17	$1,912,461.47
15	$2,369,928.75	**$580,968.82**	$1,788,959.93
16	$2,464,725.90	**$446,207.57**	$2,018,518.33
17	$2,563,314.93	$412,055.87	$2,151,259.06
18	$2,665,847.53	$428,538.11	$2,237,309.42
19	$2,772,481.43	$445,679.63	$2,326,801.80
20	$2,883,380.69	**$713,506.82**	$2,169,873.87
21	$2,998,715.92	$482,047.09	$2,516,668.83
22	$3,118,664.55	$501,328.98	$2,617,335.58
23	$3,243,411.14	$521,382.13	$2,722,029.00
24	$3,373,147.58	**$592,237.42**	$2,780,910.16
25	$3,508,073.48	$563,926.92	$2,944,146.57
		NPV	**$21,397,348.22**

Chapter 5: Results and Discussions

5.1 Technical Evaluation of Medium and High Temperature fuel cells

Based on the results obtained from the technical evaluation of SOFC and PEMFC, the optimum operating conditions were obtained in order to use these values as a reference to start analyzing the integrated system. According to the results obtained, we concluded that the fuel and air supplied to the fuel cell stack could be pressurized up to 20 bar. These results provide more flexibility in deciding the best pressure ratio for the fuel and air compressors in the integrated systems. Furthermore, the results also showed that the PEMFC fuel cell operates efficiently at a temperature of around 420 K which also helps to decide the required operating conditions when integrating the PEMFC stack into the integrated cycle.

5.2 Economic Feasibility of Fuel Cells

Based on the sensitivity analysis for the SOFC stack, the two most critical factors affecting the SOFC investment are fuel cell efficiency and electricity price. Since these two factors may result in a negative NPV, they can be considered as possible risks.

On the other hand, the economic analysis for the PEMFC showed that the most critical two factors which affect the NPV of PEMFC are the electricity price and the electrical power generated from the PEMFC. However, since none of the two factors may generate a negative NPV, the risk is minimal.

5.3 Technology Management of Systems under Study

Table 31 below shows the summary of the results obtained after performing the complete technical and economic evaluation of all the systems under study. The tabulated results show the net power output, the thermal efficiency, the capital cost, and the NPV of each of the systems under study.

Table 31: Summary of Technical and Economic Evaluations

No.	System	Total Exergy Destruction (kW)	Net Power Output (kW)	Thermal Efficiency	2nd Law Efficiency	NPV
1	Gas Turbine Cycle	566	720	54.7%	56.2%	$16,528,255.78
2	Gas Turbine+ SOFC	559	800	61%	59%	$18,317,590.15
3	Gas Turbine +SOFC+PEMFC	554	920	69%	62.4%	$21,397,348.22

As shown in the table, the integrated system with both PEMFC and SOFC was found to be the best option technically and commercially.

Figures 43 and 44 below show the summary of the obtained results.

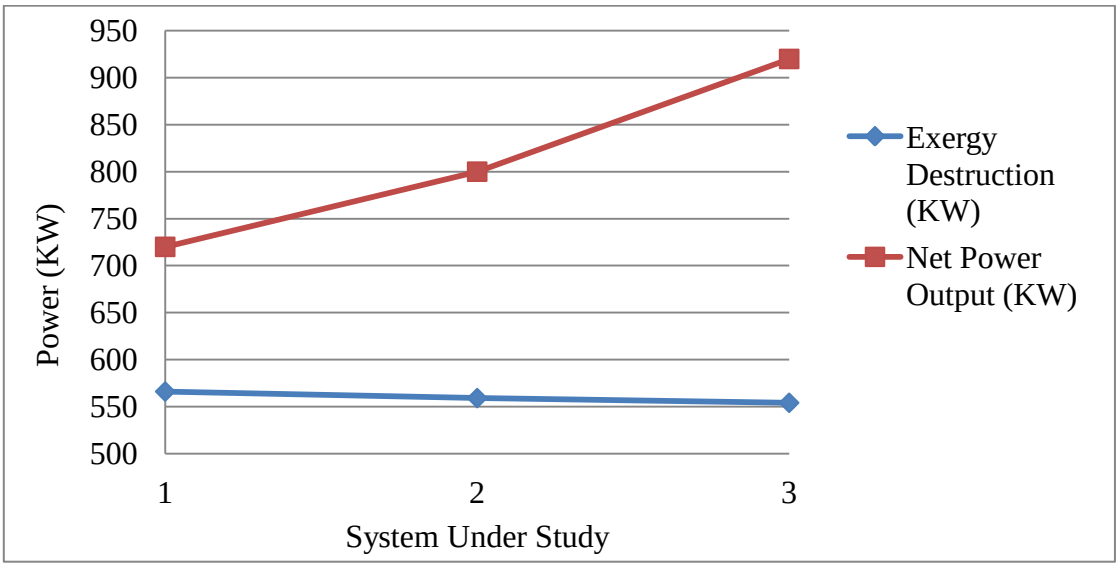

Figure 43: Comparison between Proposed Systems in terms of output power and exergy destruction

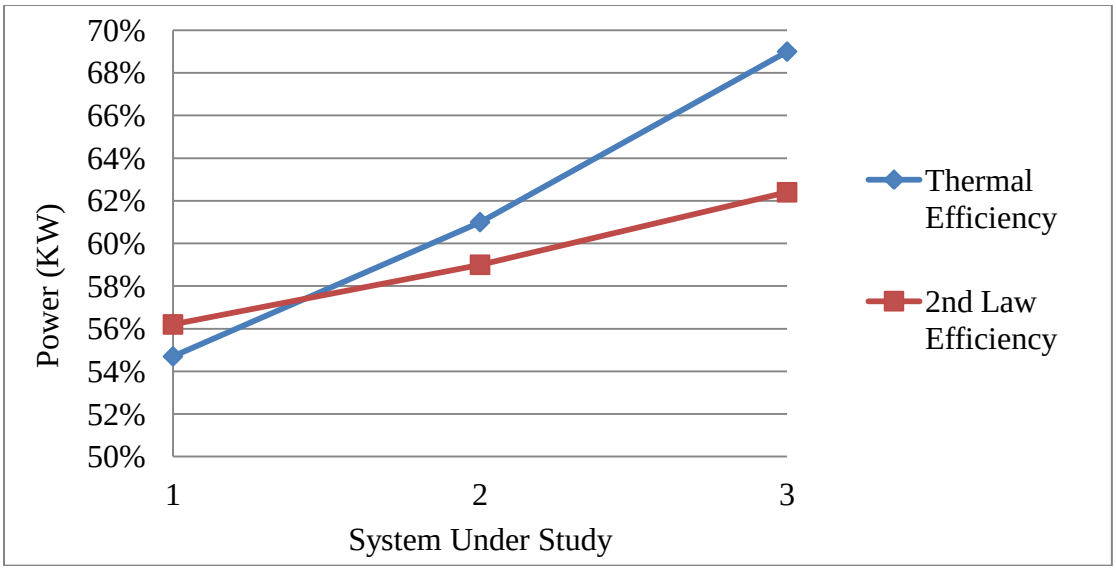

Figure 44: Comparison between Proposed Systems in terms of thermal efficiency and 2nd law efficiency

5.4 2nd Law analysis of the proposed Systems

A complete and detailed exergy analysis was performed for each of the systems under study. Based on the obtained results, we found that although the 2nd law efficiency was found to be lower for each of the proposed systems, the results were in line with the thermal analysis. The results have shown that the integrated system with both PEMFC and SOFC integrated into the gas turbine cycle has the maximum 2nd law efficiency and the lowest exergy destruction. In addition to this, the results showed that the turbine efficiency has increased after integrating the PEMFC stack due to the fact that the water contents in the flow entering the gas turbine were higher in the case of the PEMFC. This happens because of the chemical reactions in the PEMFC which produces water. Furthermore, the results also showed that the maximum exergy destruction was occurring in the combustion chamber, which supports our proposal to rely on the SOFC and heat exchangers as an additional heat source in the system.

5.5 Comparison with other related research work

Table 32 shows a brief description of the proposed systems obtained from different sources in order to compare with results obtained in this Thesis:

Table 32: Description of the proposed systems from other related research work

Sr.	Reference number	Paper title	Proposed System
1	[10]	Multi-level modeling of SOFC–gas turbine hybrid system	SOFC integrated in Gas turbine cycle
2	[24]	Thermodynamic analysis of a combined gas turbine power system with a solid oxide fuel cell through exergy	SOFC integrated in Gas turbine cycle
3	[29]	Simulation and exergy analysis of a hybrid Solid Oxide Fuel Cell (SOFC)–Gas Turbine System	Internal reforming SOFC and heat recovery steam generator integrated in gas turbine cycle
4	Current Study	Technology Management and Analysis of Integrating Fuel Cell Systems in Gas Turbine Power Plants	SOFC and PEMFC integrated in gas turbine cycle

The results and the operating conditions of each of the papers mentioned in table 32 are summarized in table 33:

Table 33: Summary of operating conditions and results from the papers under study

Case no.	Reference number	Fuel	Turbine Inlet Temperature (K)	Turbine Inlet Pressure (bar)	Thermal efficiency (%)	2nd law efficiency (%)
1	[10]	CH_4	1200 K	10	61.9%	53%
2	[24]	CH_4	1500 K	12	66%	55%
3	[29]	CH_4	1700 K	16	64%	58%
4	Current Study	CH_4	1200 K	10	65%	56%
5	Current Study	CH_4	1500 K	12	68%	60%
6	Current Study	CH_4	1700 K	16	68%	62%
7	Current Study	CH_4	2000 K	20	70%	63%

Figure 45 below shows the summary of the obtained results:

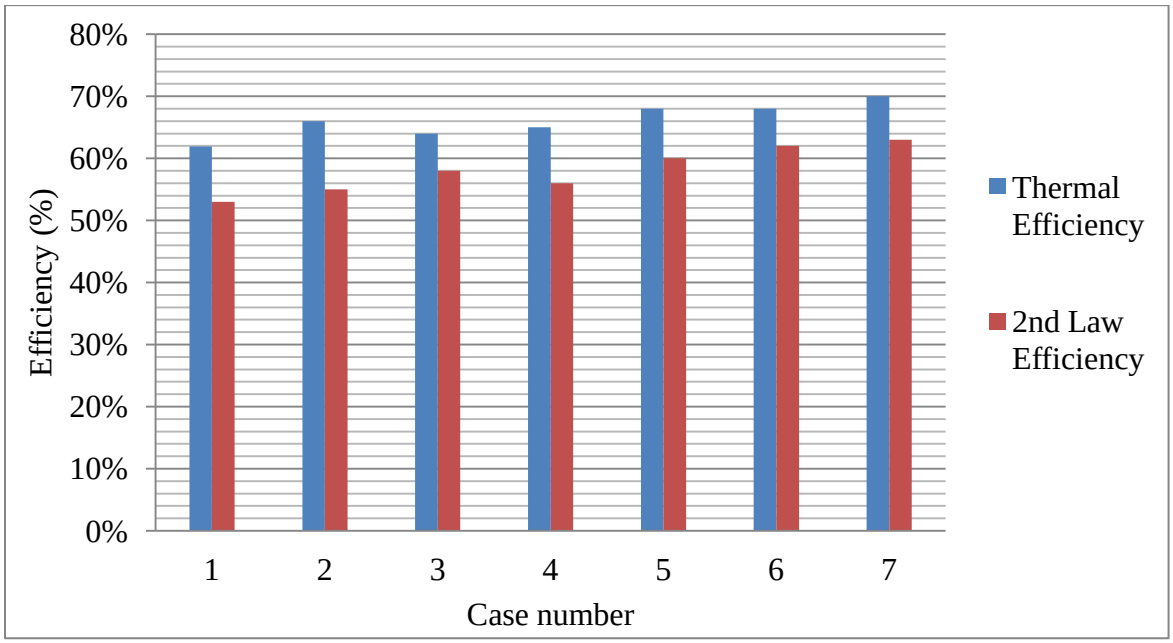

Figure 45: Summary of comparison with other related research work

Based on the comparison shown in Table 33 and Figure 45, it can be included that the maximum efficiency is obtained when integrating both the SOFC and the PEMFC in the gas turbine cycle at Turbine Inlet Temperature of 2000 K, at Turbine Inlet Pressure of 20 bars.

Chapter 6: Challenges and Conclusions

6.1 Challenges

6.1.1 Cost Reduction

In spite of the technical difficulties to be resolved to commercialize the fuel cell systems, the key issue is actually economic. Currently, the fuel cell costs about US$2000-5000 per kW, while a diesel generator costs only about US$800- $1500 per kW, and a natural gas turbine is about US$400 per kW. The materials used and the fabrication techniques applied control the cost of SOFC stacks. In addition to this, due to the fact that SOFC operates at high temperatures, an expensive material is used to build the SOFC system. Some researchers claim that it is possible to reduce the operating temperatures to use low cost materials as internal connectors and for gas manifolds, but the electrode reactions and the electrolyte resistance are both harmed when operated at lower temperatures. [31] Nowadays, the manufacturing cost is the largest portion of the total cost of the fuel cells. The SOFC stack developed by Siemens-Westinghouse was manufactured using an electrochemical vapor deposition (EVD) process which is a relatively expensive technique. In order to reduce the manufacturing cost, new technologies should be introduced and the power densities should be improved.

6.1.2 Scale-Up of Fuel Cell Module

In order to be used in power generation systems, the SOFC capacity should range from kilowatt to megawatt levels. Vendors tend to develop standard stacks of SOFC modules which can be customized to different power rating requirements. As of today, the SOFC stacks have been demonstrated to produce only hundreds of kilowatts. However, the SOFCs have not yet been demonstrated in the megawatt scale. [32] Scaling up the SOFC stack is considered a major challenge as more focus is required on the stack design, configurations, materials for long-life operation, system layout, manufacturing technique, performance of the cell, and the thermal energy management.

6.1.3 Safety and Reliability

Before applying the SOFC stack, it is important to consider the reliability of its operation and safety. In addition to this, integrating the SOFC stack is more complicated than the stand-alone operation. Integrating the SOFC in terms of the exchange of both the material and the thermal energy between the different components in the integrated cycle should be holistically evaluated. Many researchers have been working to address all the system control issues. [33] All these challenges need to be overcome in order to guarantee a safer operation in the practical conditions. Furthermore, the configurations and strategies have to be validated and improved using new demonstrations.

6.1.4 Hydrogen production

As mentioned earlier, hydrogen is an ideal fuel for different types of fuel cells. Although we have used CH_4 as a fuel for our proposed systems, the hydrogen economy is one of the most reliable ways to reduce the dependence on fossil fuels and to decrease toxic emissions. Currently, 95% of hydrogen is being produced from the reformation of natural gas and the balance is produced from electrolysis, which requires a huge amount of energy to split the water in hydrogen and oxygen.[33] Both these methods are still expensive and more research and technological advancement is needed. As a matter of fact, splitting the water to produce hydrogen can be done using more economic ways like the radio-frequency method proposed by John Kanzuis [36]. Moreover, more effort has to be put into improving hydrogen storage techniques.

6.2 Conclusions

The obtained results show a great advantage of introducing the use of the PEMFC stack in the combined cycle including an SOFC. The PEMFC stack utilizes the excess of hydrogen produced by the SOFC stack as a fuel. Furthermore, another important advantage is that the water contents of the gas mixture entering the turbine which is coming from the reactions in the PEMFC decreases the temperature in the interior of the turbine, which allows it to gain more efficiency via increasing the temperature of the fuel combustion. In addition to this, the simulation results clearly indicate the advantage of operating the fuel cell stack in the high pressure region, as the PEMFC stack is capable of

operating 20% higher than its nominal efficiency. In addition, it also runs at a higher operating temperature. Because of this, less energy will be required to cool the flow leaving the SOFC and also the amount of energy required to run the combustor will be less. The economic evaluation of the system clearly shows the advantage of introducing the fuel cell technology in a gas turbine cycle. As the results show, the efficiency of the proposed system is 15% higher than the conventional gas turbine system, with more economic value.

References

[1] G. Hoogers. “The Fueling Problem: Fuel Cell Systems” in *Fuel Cell Technology Handbook*. Danvers, MA: CRC Press, 2003, pp. 125-148.

[2] Y. Cengel, M. Boles. *Thermodynamics: An Engineering Approach.* Manhattan, NY: McGraw Hill, 2001, pp. 450-520.

[3] Y. Ma, G. Karady, A. Winston III, P. Gilbert, R. Hess, D. Pelley. “Economic feasibility prediction of the commercial fuel cells.” *Energy Conversion and Management*, vol. 50, pp. 422-430, February 2009.

[4] X. Zhang, S. Chan, G. Li, H. Ho, Jun Li, Z. Feng. "A review of integration strategies for solid oxide fuel cells." *Journal of Power Sources*, vol. 195, pp. 685-702, February 2010.

[5] Y. Yi, A. D. Rao, J. Brouwer, G. Samuelsen. "Fuel flexibility study of an integrated 25kW SOFC reformer system." *Journal of Power Sources*, vol. 144, pp. 67-76, June 2005.

[6] Y. Haseli, I. Dincer, G.F. Naterer. "Thermodynamic modeling of a gas turbine cycle combined with a solid oxide fuel cell." *International Journal of Hydrogen Energy*, vol. 33, pp. 5811-5822, October 2008.

[7] K. Tanaka, C. Wen, K. Yamada. ” Design and evaluation of combined cycle system with solid oxide fuel cell and gas turbine.” *Fuel*, vol. 79, pp. 1493-1507, October 2000.

[8] S. Yerramalla , A. Davari , A. Feliachi , T. Biswas. “Modeling and simulation of the dynamic behavior of a polymer electrolyte membrane fuel cell.” *Journal of Power Sources*, vol. 124, pp. 104-113, October 2003.

[9] C. Spiegel. *PEM Fuel Cell Modeling and Simulation Using Matlab*. Burlington, MA: Elsevier Inc., 2008, pp. 365-405.

[10] S.H. Chan, H.K. Ho, Y. Tian. "Multi-level modeling of SOFC–gas turbine hybrid system." *International Journal of Hydrogen Energy*, vol. 28, pp. 889-900, May 2002.

[11] C. Winter. "Into the hydrogen energy economy—milestones." *International Journal of Hydrogen Energy*, vol. 30, pp. 681-685, July 2005.

[12] A. Avadikyan, P. Cohendet. *The Economic Dynamics of Fuel Cell Technologies.* Berlin, Germany: Springer-Verlag, 2010, pp. 43-111.

[13] E. Bompard, R. Napoli, B. Wan, G. Orsello. "Economics evaluation of a 5 kW SOFC power system for residential use." *International Journal of Hydrogen Energy*, vol. 33, pp. 3243-3247, June 2008.

[14] S. Ang, E. Fraga, N.P. Brandon, N.J. Samsatli, D. Brett. "Fuel cell systems optimization Methods and strategies." *International Journal of Hydrogen Energy*, vol. 36, pp. 14678-14703, November 2011.

[15] T.E. Lipman, J.L. Edwards, D.M. Kammen. "Fuel cell system economics: comparing the costs of generating power with stationary and motor vehicle PEM fuel cell systems." *Energy Policy*, vol. 32, pp. 101-123, January 2004.

[16] P. Agnolucci. "Economics and market prospects of portable fuel cells." *International Journal of Hydrogen Energy*, vol. 32, pp. 4319-4328, December 2007.

[17] F. Barbir and T. Gomez. "Efficiency and Economics of Proton Exchange Membrane (PEM) Fuel Cells." *International Journal of Hydrogen Energy*, vol. 21, pp. 891-901, October 1996.

[18] D.F. Cheddie, R.Murray. “Thermo-economic modeling of a solid oxide fuel cell/gas turbine power plant with semi-direct coupling and anode recycling.” *International Journal of Hydrogen Energy*, vol. 35, pp. 11208-11215, October 2010.

[19] A. Kazim. “Exergoeconomic analysis of a PEM fuel cell at various operating conditions.” *Energy Conversion and Management*, vol. 46, pp. 1073-1081, May 2005.

[20] M. Sreeramulu, A. Gupta, T. Srinivas. “Exergy Analysis of Gas Turbine – Fuel cell based combined Cycle Power Plant.” International Journal of Engineering Science and Technology, vol. 3, pp. 5227-5236, June 2011.

[21] A. Baheta, S. Gilani. “Exergy Based Performance Analysis of a Gas Turbine at Part Load Conditions.” *Journal of Applied Sciences,* vol. 11, pp. 1994-1999, April 2011.

[22] N. M. Jubeh. “Exergy Analysis and Second Law Efficiency of a Regenerative Brayton Cycle with Isothermal Heat Addition.” *Entropy*, vol. 7, pp. 172-187, July 2005.

[23] P.G. Bavarsad. “Energy and exergy analysis of internal reforming solid oxide fuel cell–gas turbine hybrid system.” *International Journal of Hydrogen Energy*, vol. 32, pp. 4591-4599, December 2007.

[24] Y. Haseli, I. Dincer, G.F. Naterer. “Thermodynamic analysis of a combined gas turbine power system with a solid oxide fuel cell through exergy.” *Themochimica Acta*, vol. 480, pp. 1-9, December 2008.

[25] N. Hotz, M. Lee, C.P. Grigoropoulos, S.M. Senn, D. Poulikakos. “Exergetic analysis of fuel cell micropowerplants fed by methanol.” *International Journal of Heat and Mass Transfer*, vol. 49, pp. 2397-2411, July 2006.

[26] M.M. Hussain, J.J. Baschuka, X. Li, I. Dincer. “Thermodynamic analysis of a PEM fuel cell power system.” *International Journal of Thermal Sciences*, vol. 44, pp. 903-911, September 2005.

[27] A.V. Akkayaa, B. Sahinb, H.H. Erdema. “Exergetic performance coefficient analysis of a simple fuel cell system.” *International Journal of Hydrogen Energy*, vol. 32, pp. 4600-4609, December 2007.

[28] N. Hotz, S.M. Senn, D. Poulikakos. “Exergy analysis of a solid oxide fuel cell micropowerplant.” *Journal of Power Sources*, vol. 158, pp. 333-347, July 2006.

[29] F. Calisea, M.D. d’Accadiaa, A. Palomboa, L. Vanolib. "Simulation and exergy analysis of a hybrid Solid Oxide Fuel Cell (SOFC)–Gas Turbine System." *Energy*, vol. 31, pp. 3278-3299, December 2006.

[30] A. Kazim. “Exergy analysis of a PEM fuel cell at various operating conditions.” *Energy Conversion and Management*, vol. 45, pp. 1949-1961, May 2004.

[31] K. Schootsa, G.J. Kramerb, B.C.C. van der Zwaana. “Technology learning for fuel cells: An assessment of past and potential cost reductions.” *Energy Policy*, vol. 38, pp. 2887-2897, June 2010.

[32] S. C. Ang, E.S. Fraga, N.P. Brandon, N.J. Samsatli, D. Brett. “Fuel cell systems optimisation – Methods and strategies.” *International Journal of Hydrogen Energy*, vol. 36, pp. 14678-14703, November 2011.

[33] C. Winter. “Into the hydrogen energy economy—milestones.” *International Journal of Hydrogen Energy*, vol. 30, pp. 681-685, July 2005.

[34] P. Zegers. “Fuel cell commercialization: The key to a hydrogen economy.” *Journal of Power Sources*, vol. 154, pp. 487-502, March 2006.

[35] K. Sopiana, W. Daudb. “Challenges and future developments in proton exchange membrane fuel cells.” *Renewable Energy*, vol. 31, pp. 719-727, April 2006.

[36] S. Barrett. “Progress in the European Hydrogen & Fuel Cell Technology Platform.” *Fuel Cells Bulletin*, vol. 2005, pp. 12-17, April 2005.

[37] D. Hart. “Sustainable energy conversion: fuel cells - the competitive option?.” *Journal of Power Sources*, vol. 86, pp. 23-27, March 2000.

[38] J. Wee. “Applications of proton exchange membrane fuel cell systems.” *Renewable and Sustainable Energy Reviews,* vol. 11, pp. 1720-1738, October 2007.

Vita

Nabil Omar Al Aid was born on February 26, 1986, in Riyadh, Saudi Arabia. He was educated in local public schools and graduated from Private Modern School as an honors student in 2003. He joined the American University of Sharjah in 2003 from which he graduated in 2008 after obtaining a Bachelor of Science in Electrical Engineering and a Bachelor of Science in Mechanical Engineering.

After graduation, Mr. Al Aid joint Honeywell Middle East and worked as a technical trainer. He then began a Master's program in Engineering Systems Management at the American University of Sharjah in 2009. He was awarded the Master of Science degree in Engineering Systems Management in 2013.

Mr. Al Aid has been working as a Regional Sales Manager at Honeywell Middle East since 2010.